Application of single-layer particle tracking for radiation field decomposition and interaction point reconstruction at MoEDAL

Declan Garvey, Benedikt Bergmann, Petr Mánek, Stanislav Pospíšil, Petr Smolyanskiy,

On behalf of MoEDAL

Declan.Garvey@utef.cvut.cz

Timepix3: Radiation Imaging Detector

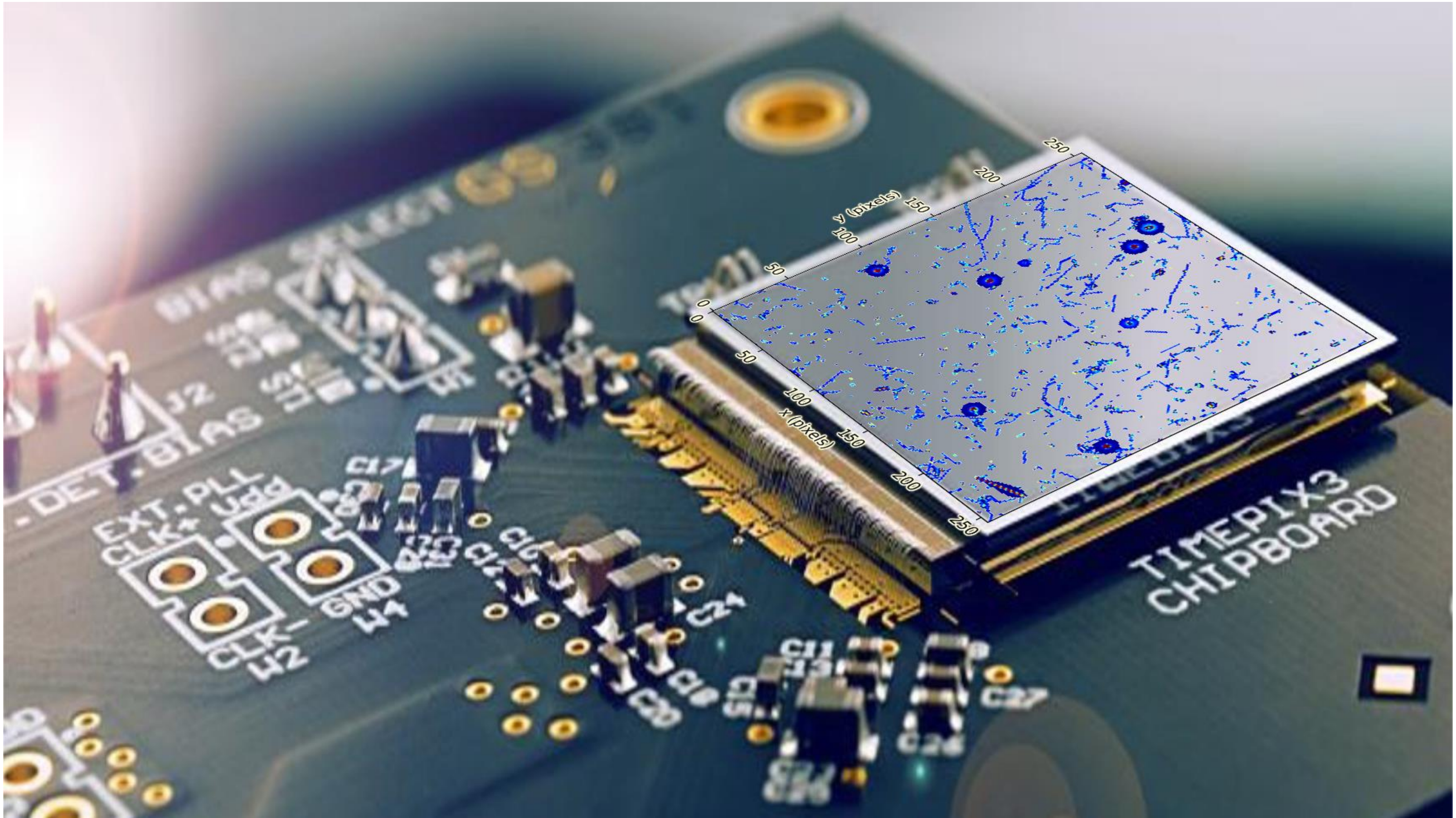

Timepix and Timepix3

- 256 x 256 pixels with 55 µm pitch (1.98 cm^2)
- Sensor layer (silicon, GaAs, CdTe, …) flip-chip bump bonded to the ASIC

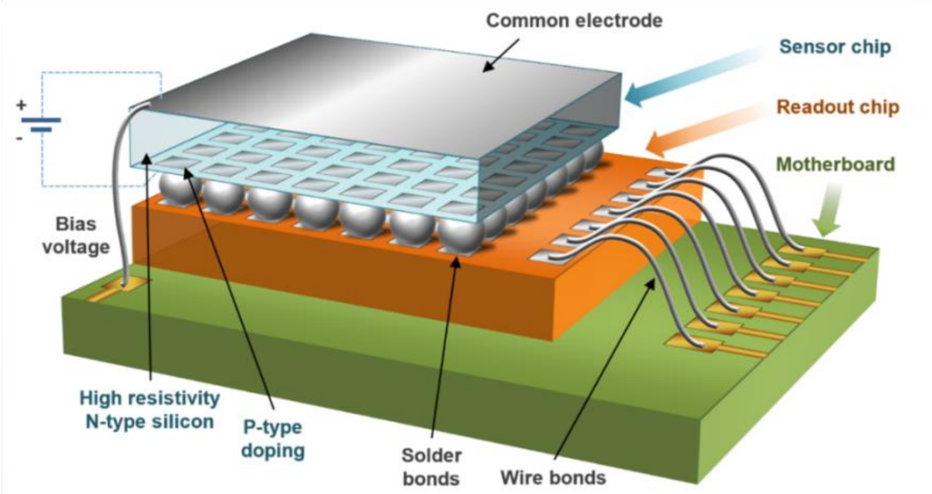

Timepix

- Frame-based readout (92 fps) – dead time > 11 ms
  - ⇨ Information is read out on a frame-by-frame basis
- Measurement of energy **or** time (Δt = 20.8 ns)
- Minimal detectable energy: ~ 3.5 keV

Timepix3

- Data-driven readout (max. count rate 40 Mpix/s)
  - ⇨ Pixels are continuously read out throughout the entire measurement
- Per pixel dead time: 475 ns
- Measurement of energy **and** time (Δt = 1.56 ns)
- Minimal detectable energy per pixel: 3 keV

Timepix3 with chipboard

Particle Tracking by Connecting the Dots

- Traditionally, particle tracking is performed using multiple layers of thin detectors
- Tracking information is then calculated by recording coincidence measurements in each detector and "connecting the dots"

So, the question is:

Can we achieve similar results using only a single-layer detector?

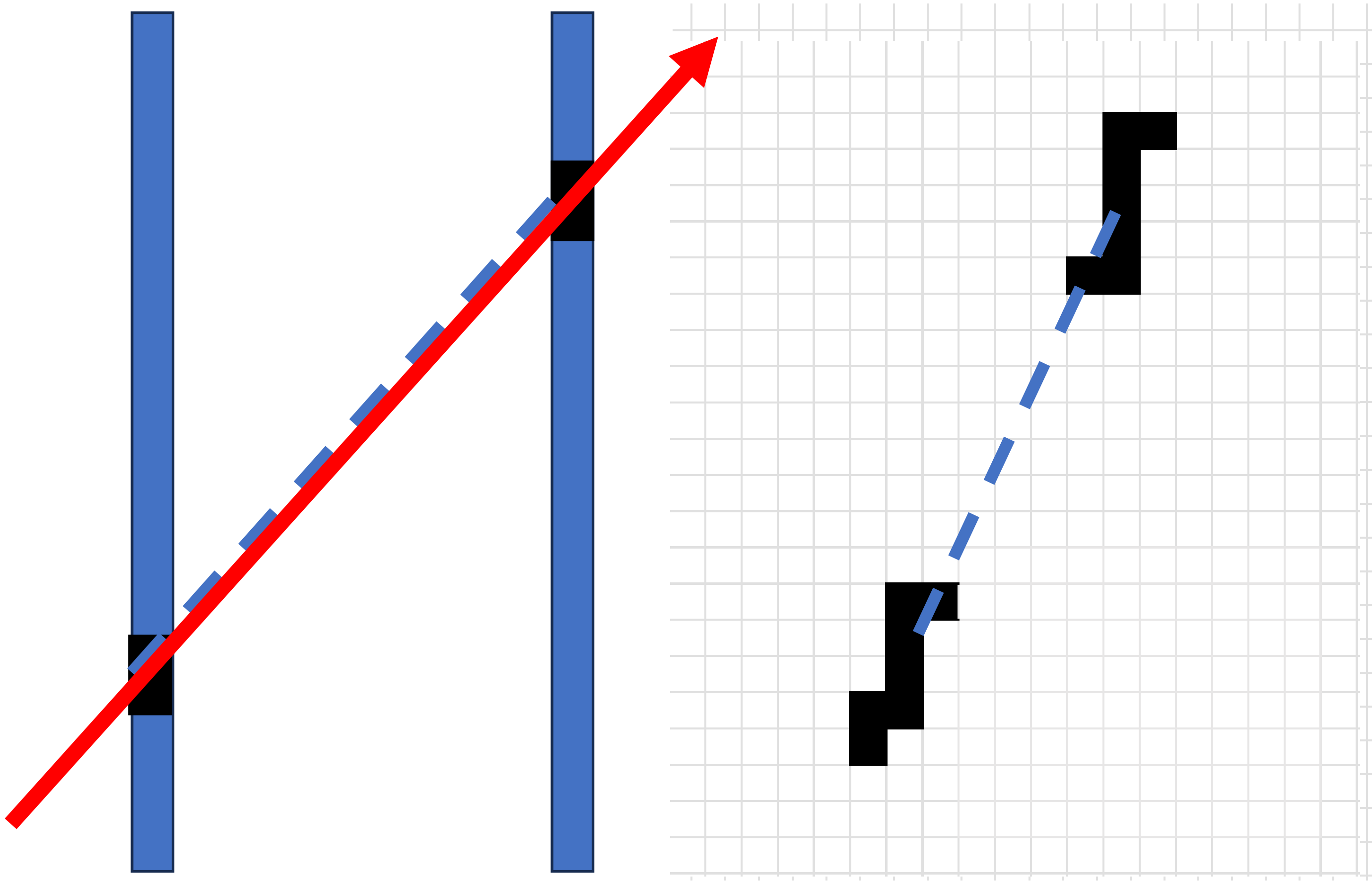

Solid-State Time-Projection Chamber:

3D Reconstruction of Particle Tracks

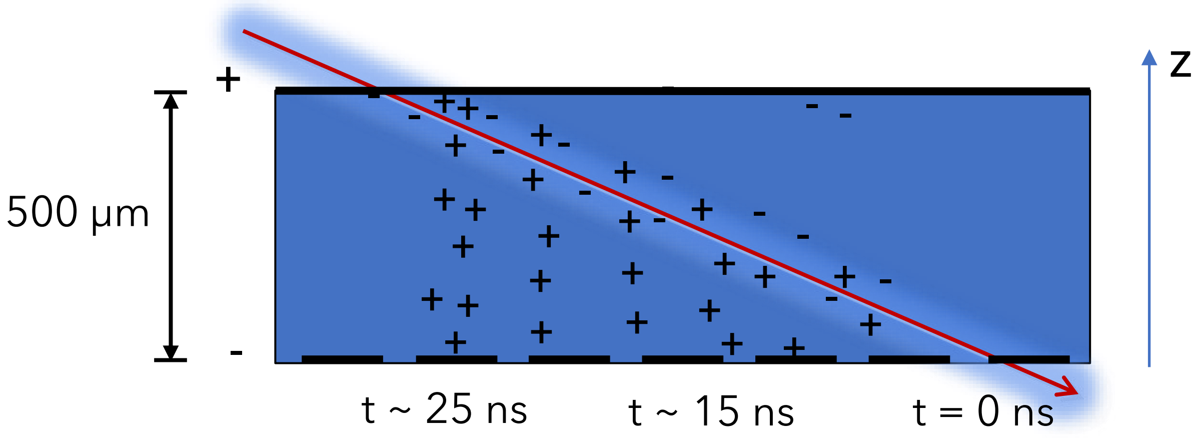

2000 µm, pixel pitch: 55 µm

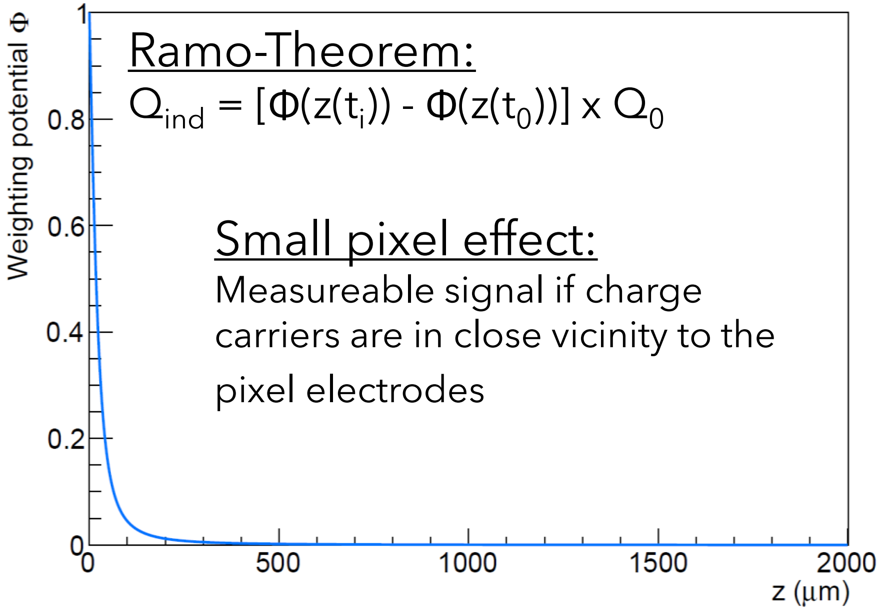

<u>Ramo-Theorem:</u>

$Q_{ind} = [\Phi(z(t_i)) - \Phi(z(t_0))] \times Q_0$

<u>Small pixel effect:</u>

Measureable signal if charge carriers are in close vicinity to the pixel electrodes

<u>Charge carrier drift motion:</u>

e^- and h^+ drift described by

$$v_e = -\mu_e \times E(z)$$
$$v_h = \mu_h \times E(z)$$

$\mu_{e/h}$: Mobility of e^-/h^+

<u>Electric field parametrisation:</u>

Si: $\vec{E}(z) = \frac{U_B}{d}\vec{e_z} + \frac{2U_{dep}}{d^2}\left(\frac{d}{2} - z\right)\vec{e_z}$;

CdTe: $\vec{E}(z) = \frac{U_B}{d}\vec{e_z}$

U_B: Bias voltage; U_{dep}: Depletion voltage; d: Sensor thickness

→ Look up table: $z(t_{meas.}, E_{meas.})$

Bergmann et al. Eur. Phys. J. C (2017) 77: 421. https://doi.org/10.1140/epjc/s10052-017-4993-4
Bergmann et al., Eur. Phys. J. C (2019) 79: 165. https://doi.org/10.1140/epjc/s10052-019-6673-z

3D Tracking in 500 μm Si Timepix3

120 GeV/c pion tracks accompanied by δ-rays measured at SPS:

z-resolution:
σ_z ~30 μm

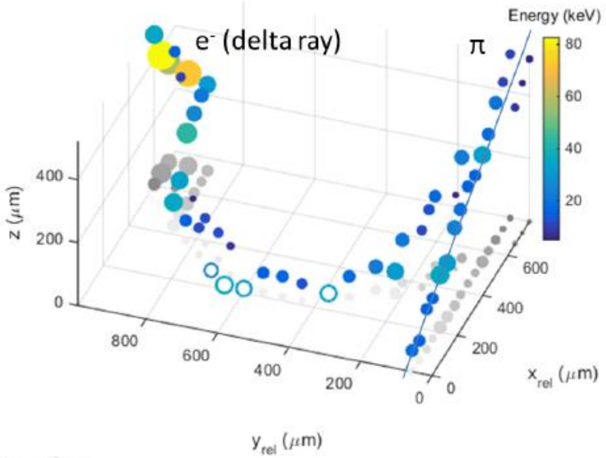

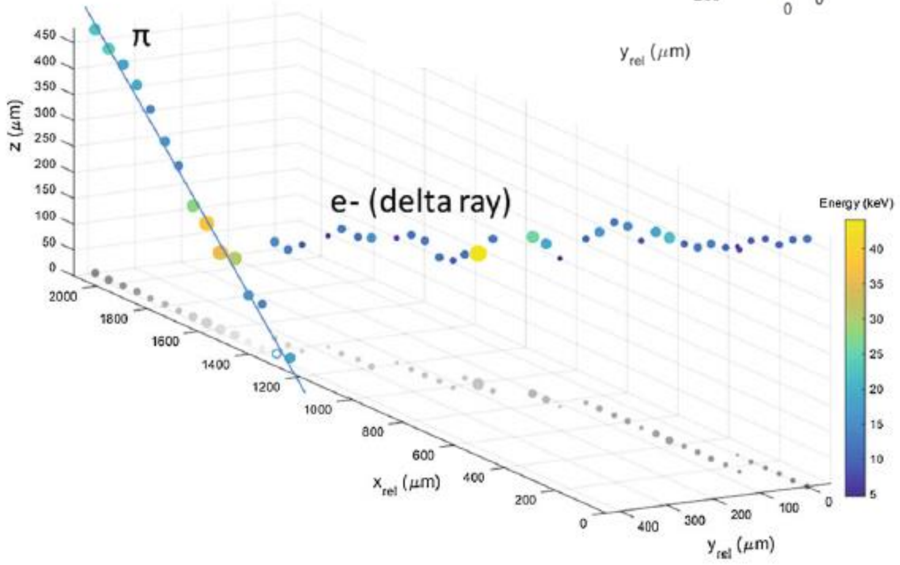

A cosmic μ measured in the Prague laboratory:

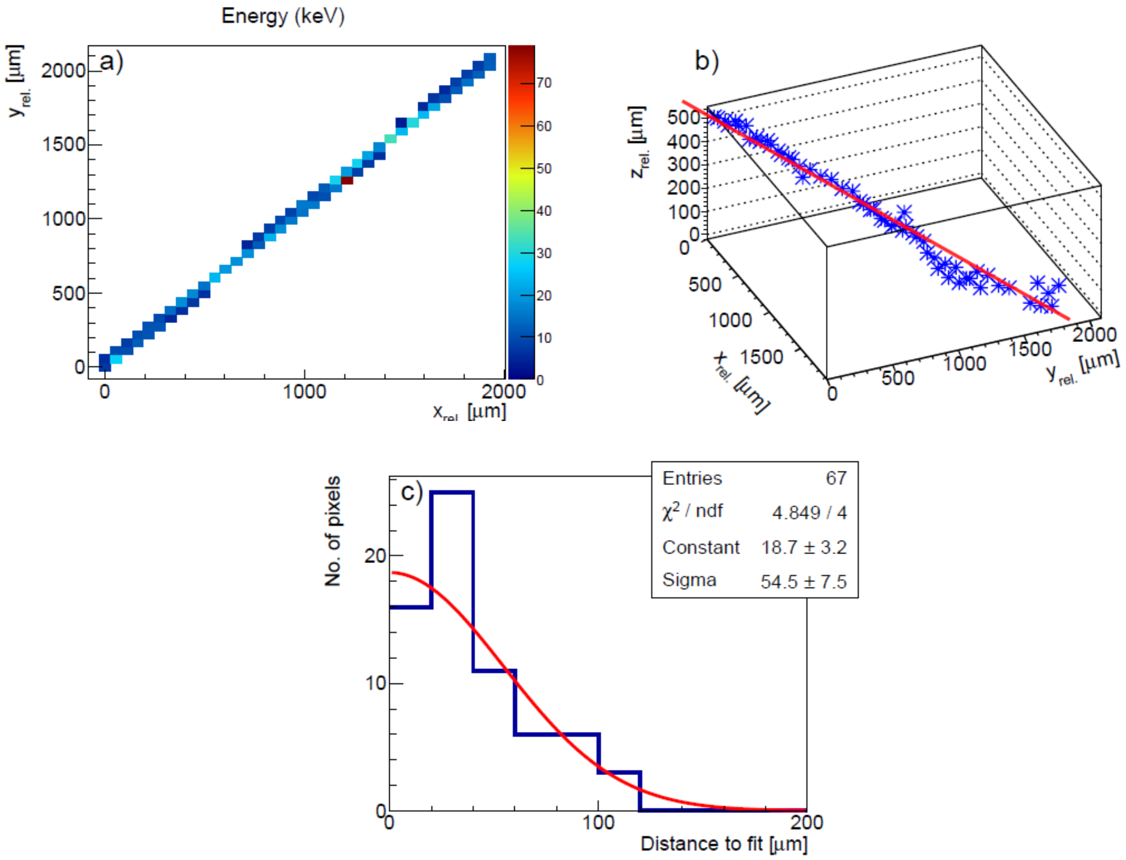

Bergmann et al. Eur. Phys. J. C (2017) 77: 421.
https://doi.org/10.1140/epjc/s10052-017-4993-4

Energy Deposition Spectra of Charged Energetic Particles

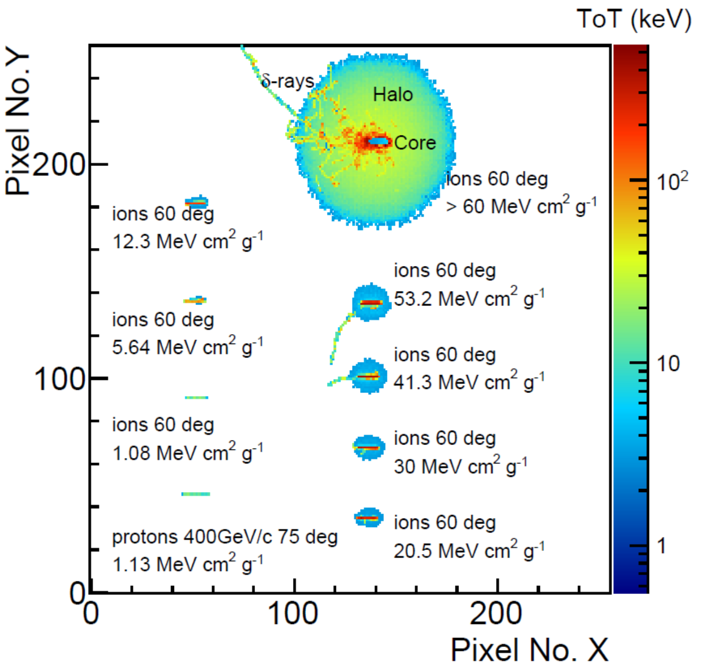

Different track shapes observed in a mixed relativistic ion beam 330 GeV/c Pb on target

Energy loss of energetic charged particles described by Landau-Vavilov distribution with Gaussian smearing

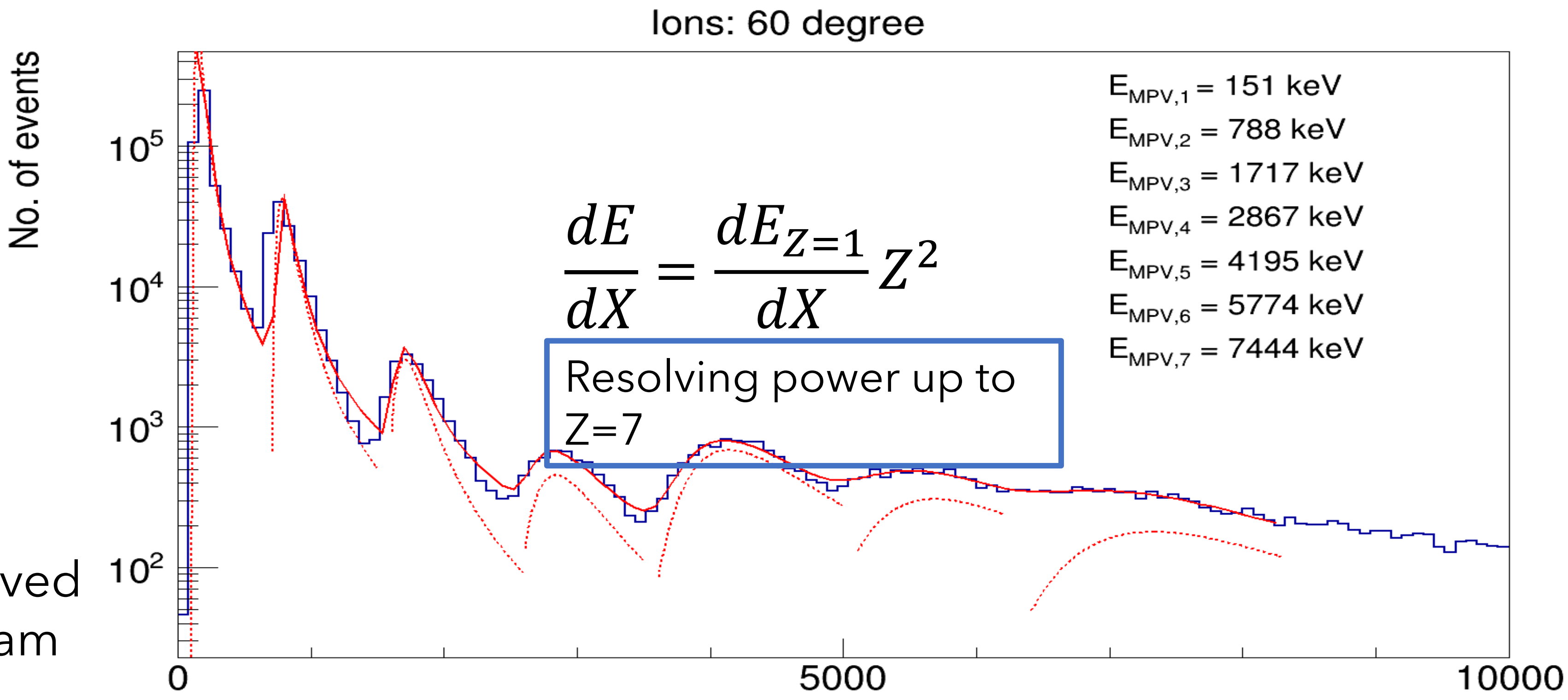

$$\frac{dE}{dX} = \frac{dE_{Z=1}}{dX} Z^2$$

Resolving power up to Z=7

P. Smolyanskiy *et al.* *JINST* **16** P01022, 2021. https://dx.doi.org/10.1088/1748-0221/16/01/P01022

Single-Layer Particle Tracking in MoEDAL

Timepix3 in MoEDAL at Run 2 – Feasibility Study

Installation of two Timepix3 detectors in MoEDAL in **September 2018**. Timepix3 are placed at 1.1 m distance to IP8 with a relatively unobstructed view

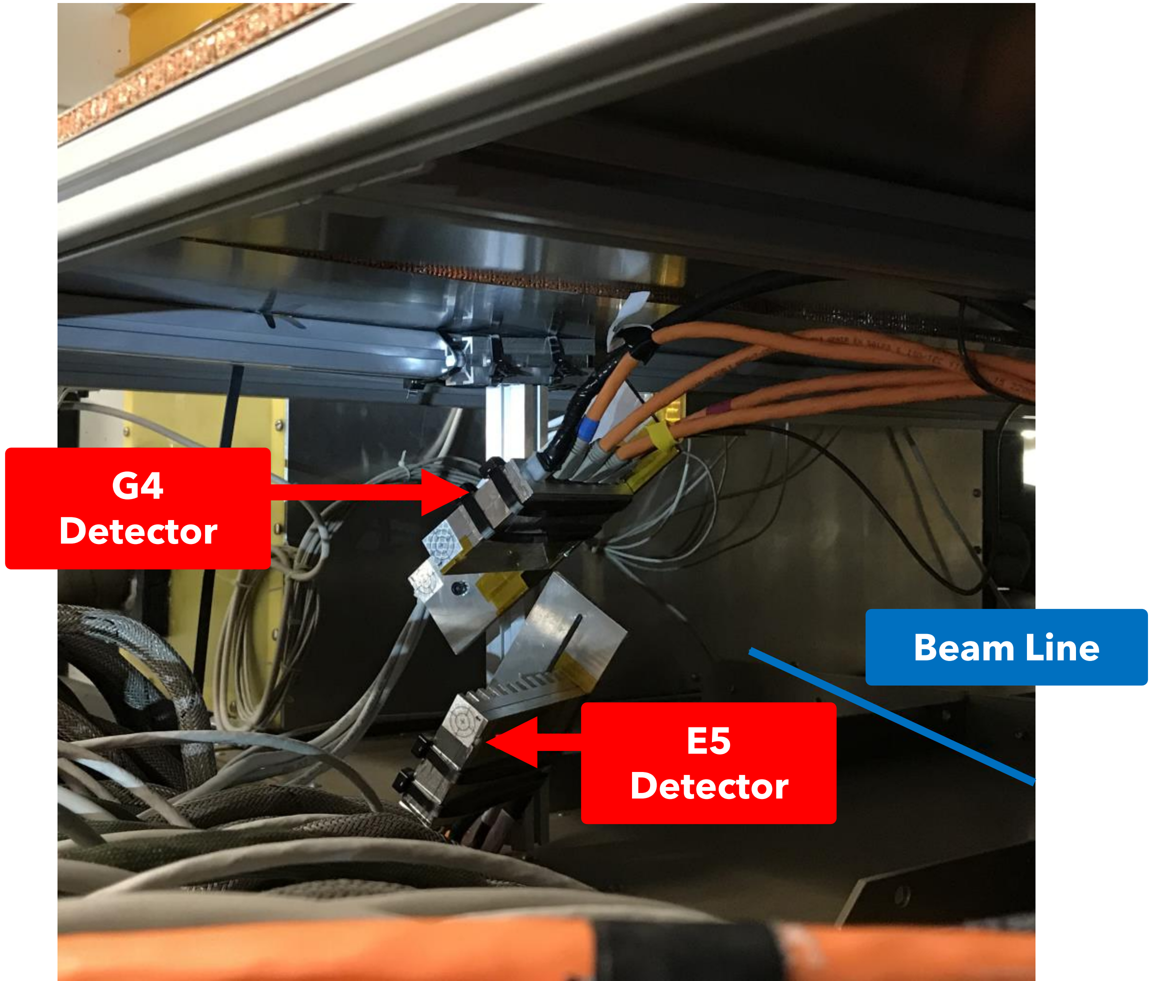

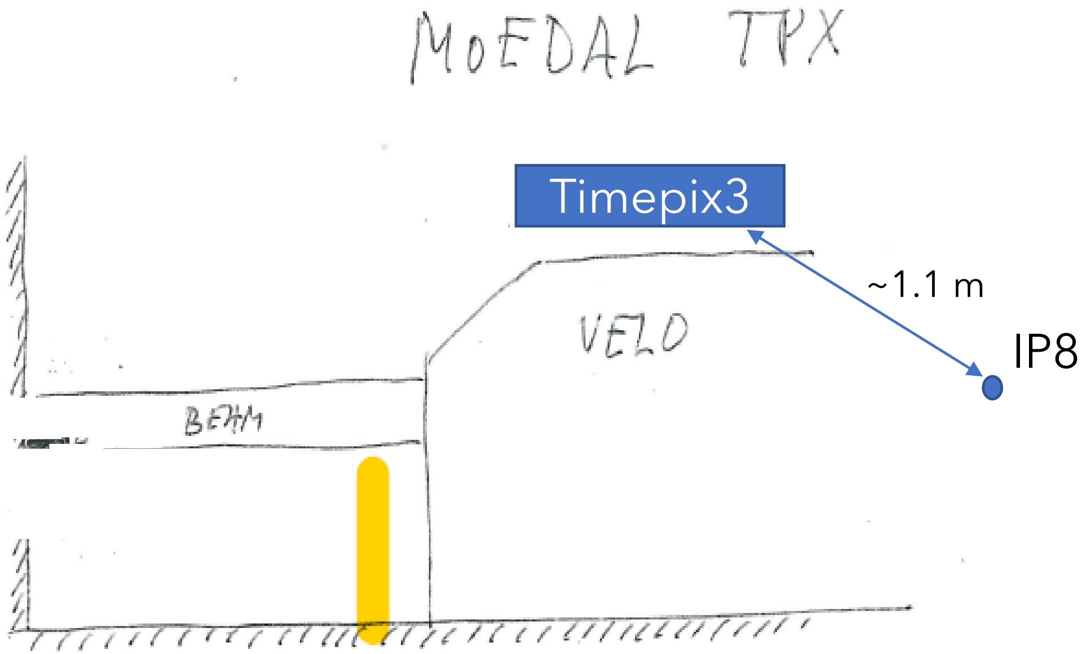

Continuous quasi dead-time free measurement (in real time) keeping a permanent record of **all particle traces**

- Tracking and identification of **all** particles
- Online outlier detection to search for exotics (highly ionising events)
- Bunch-by-bunch luminosity measurement
- Search for exotic signatures, e.g., "soup" events requiring timing information

Radiation Levels and Radiation Field

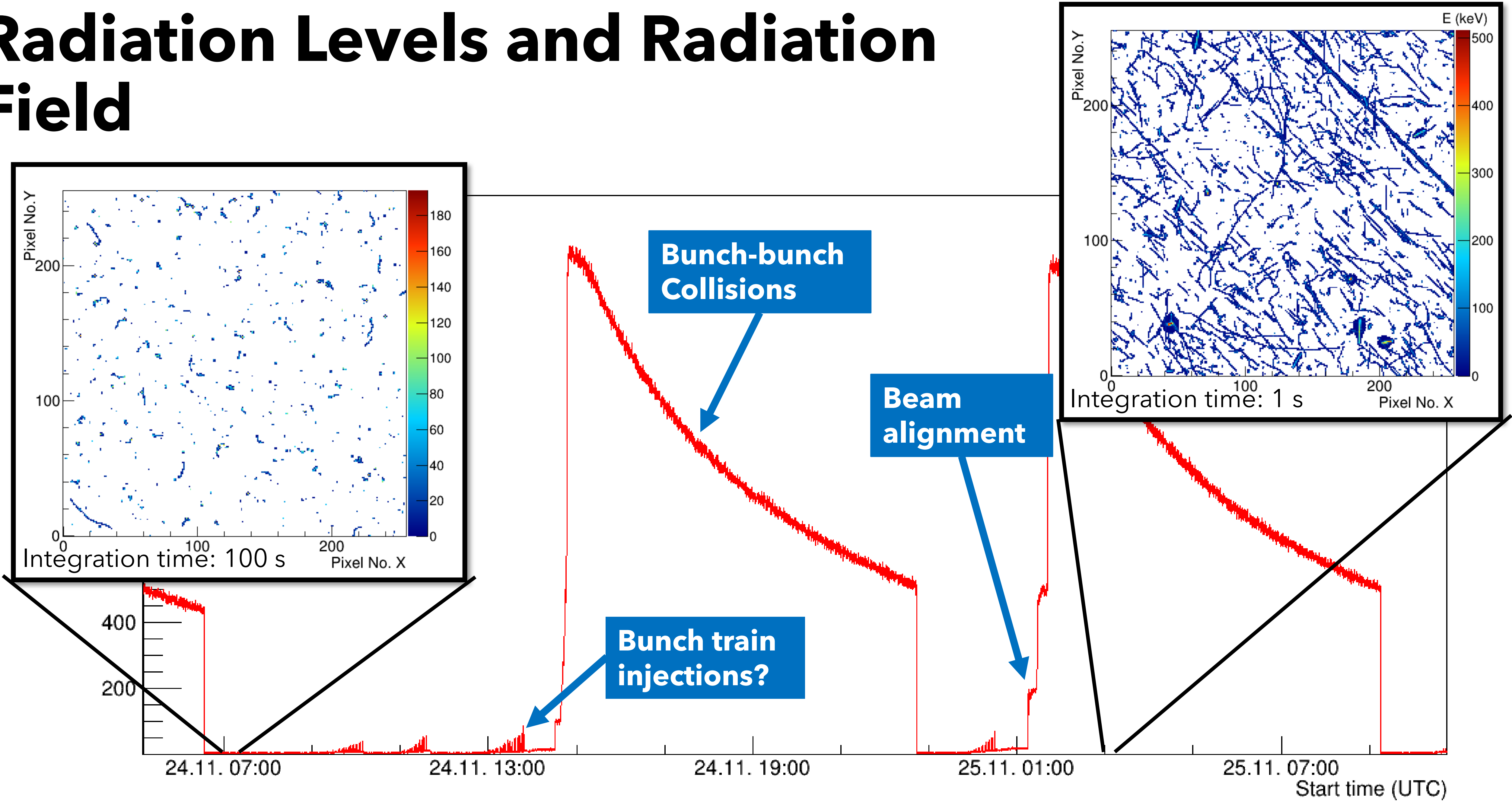

Theta Predictor Model

- To reduce the complexity of the problem, only the following two incidence angles are predicted: Azimuthal and perpendicular. Reducing it to regression problem
- **Datasets used for model development:**
  - ➪ 0.01-10 MeV electrons (curly tracks)
  - ➪ 10-500 MeV protons (thick, straight tracks)
  - ➪ 40 GeV pions (thin, straight tracks)
- It was found through an extensive study that a Random Forrest Regressor with a selection of input features produced optimal results

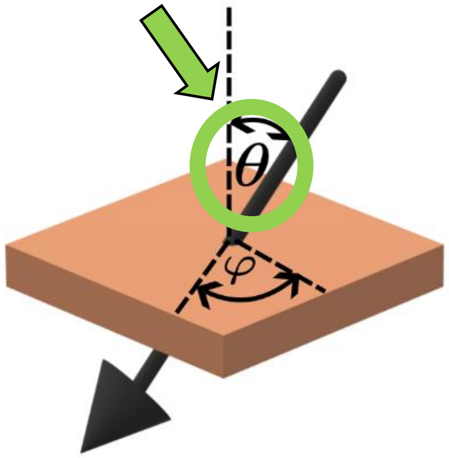

Input Features:

1. Size [no. of pixels]
2. Line standard deviation
3. Box dimensions
4. End point distance

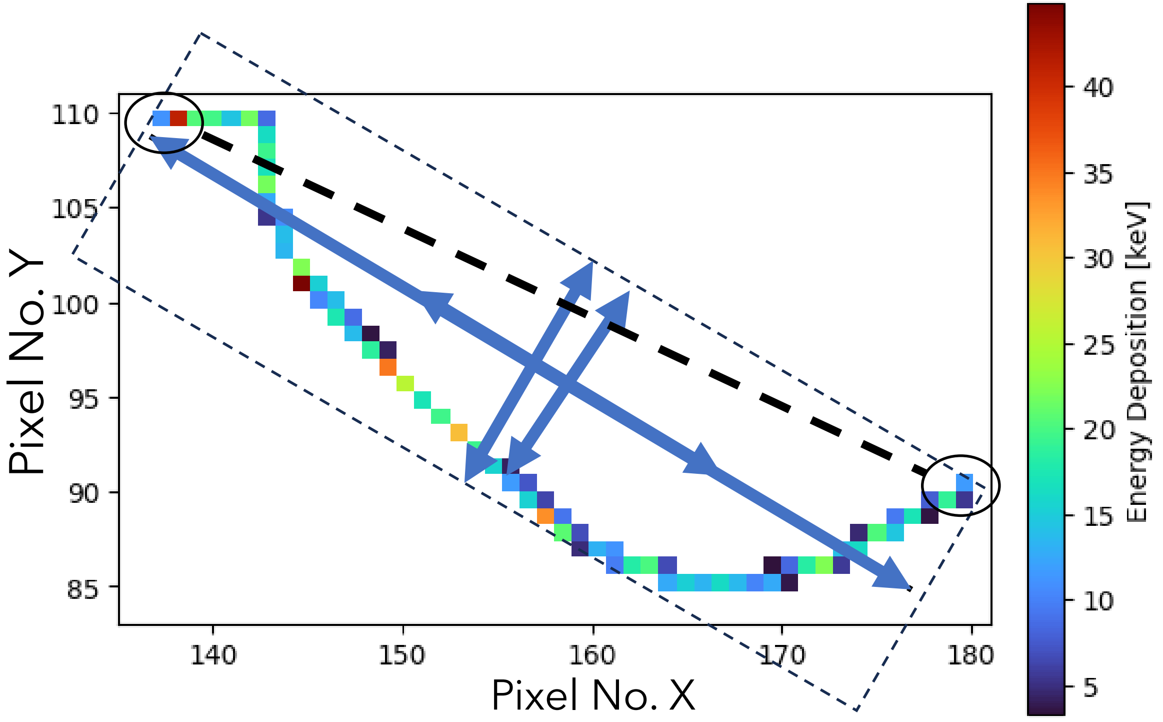

Theta Prediction Results

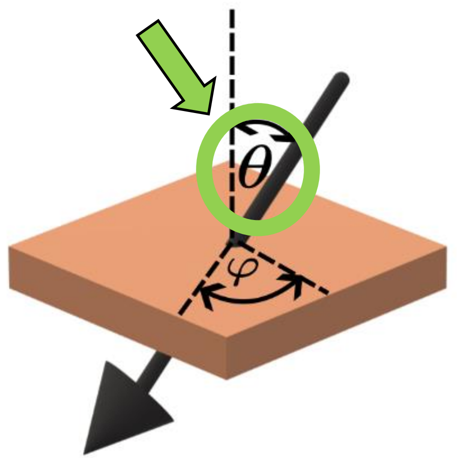

For testing separate simulation datasets were created

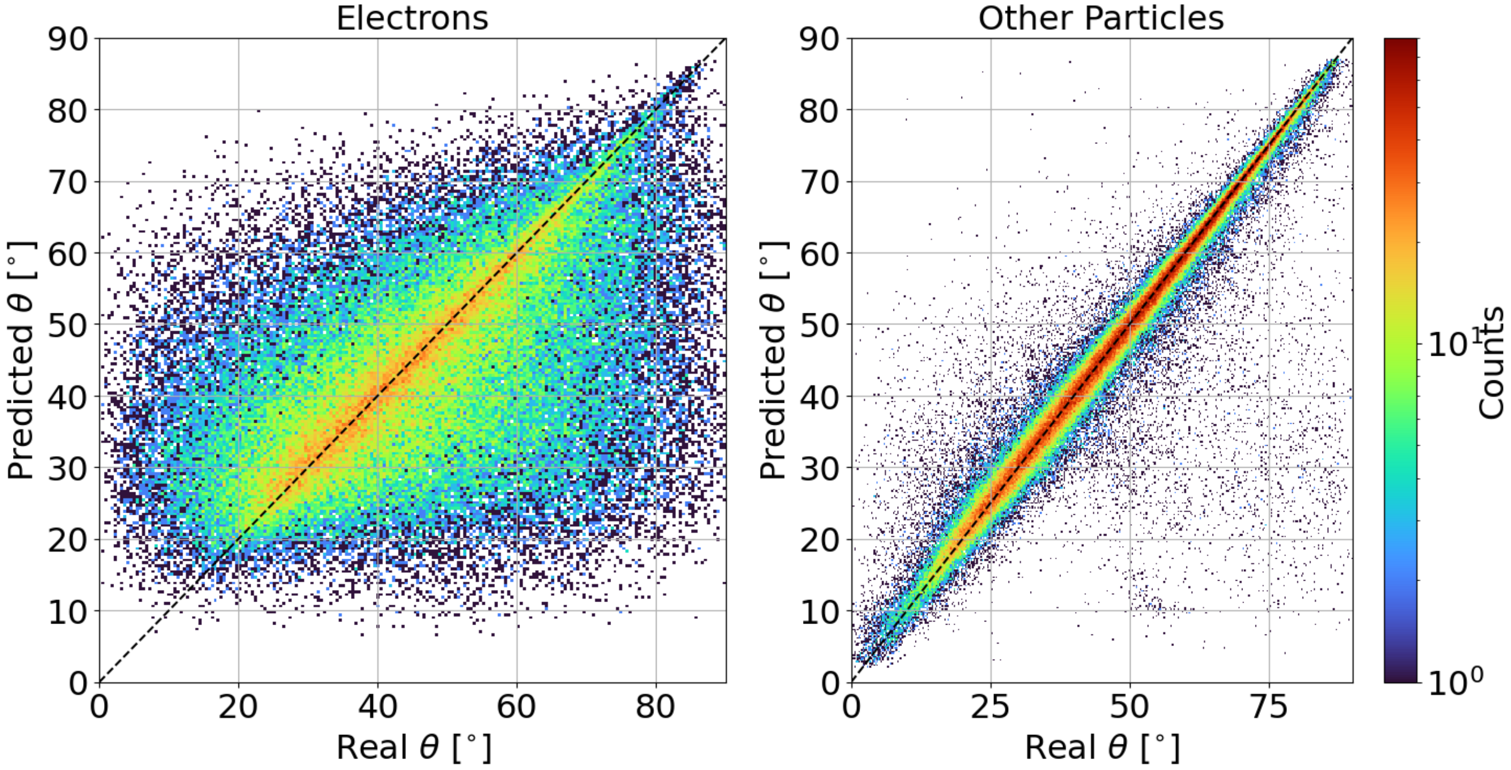

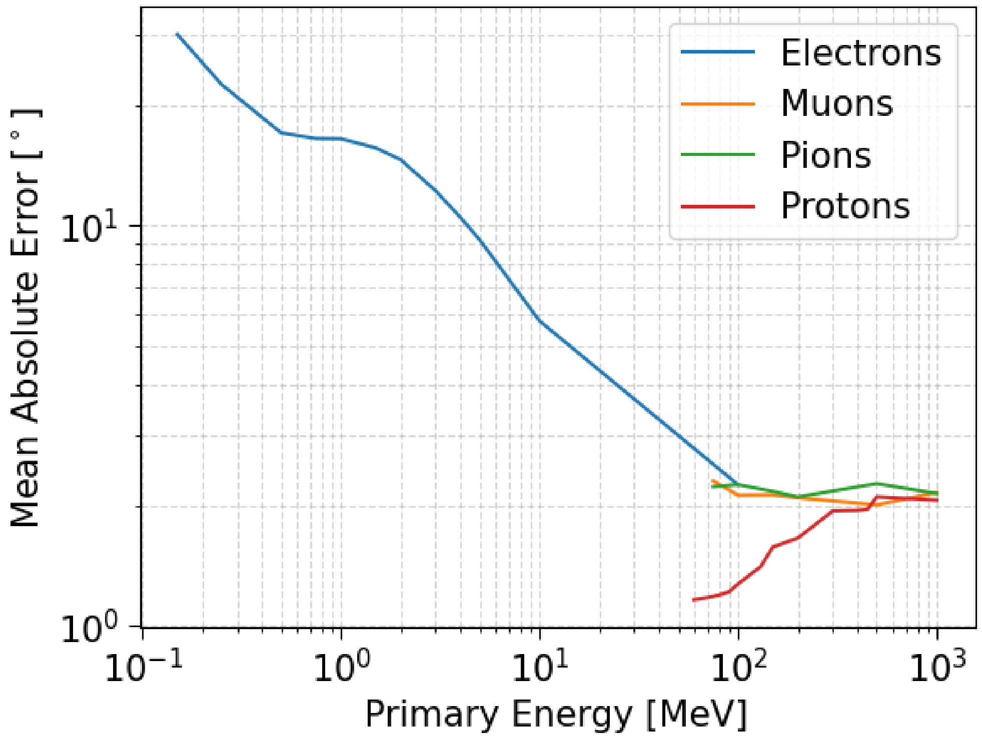

Phi Determination

- An analytic approach was used as no improvement using machine learning algorithms was achieved
- Following an extensive study, Time of Arrival [ToA] weighted averaging was found to produce the most accurate results*
- In this method, we utilise the effect that drift time within the sensor has on ToA to approximate the “mean” entry and exit points

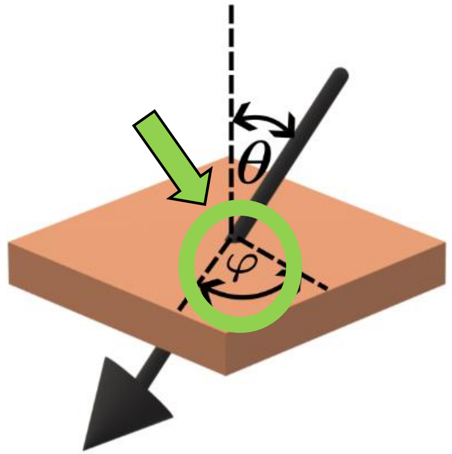

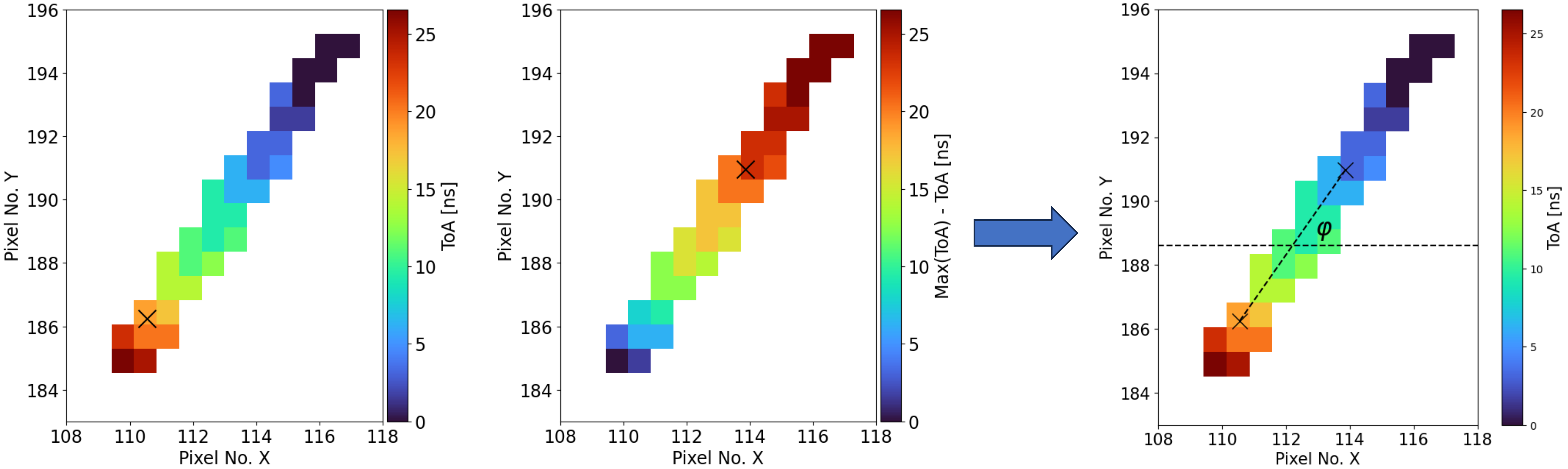

*P. Mánek et al. In: Journal of Instrumentation (2022), p. C01062. https://dx.doi.org/10.1088/1748-0221/17/01/C01062

Phi Model Results

For testing separate simulation datasets were created

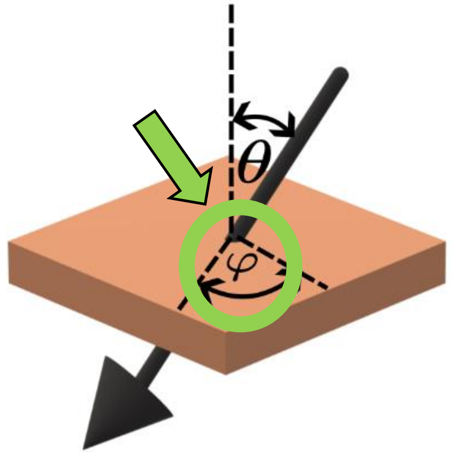

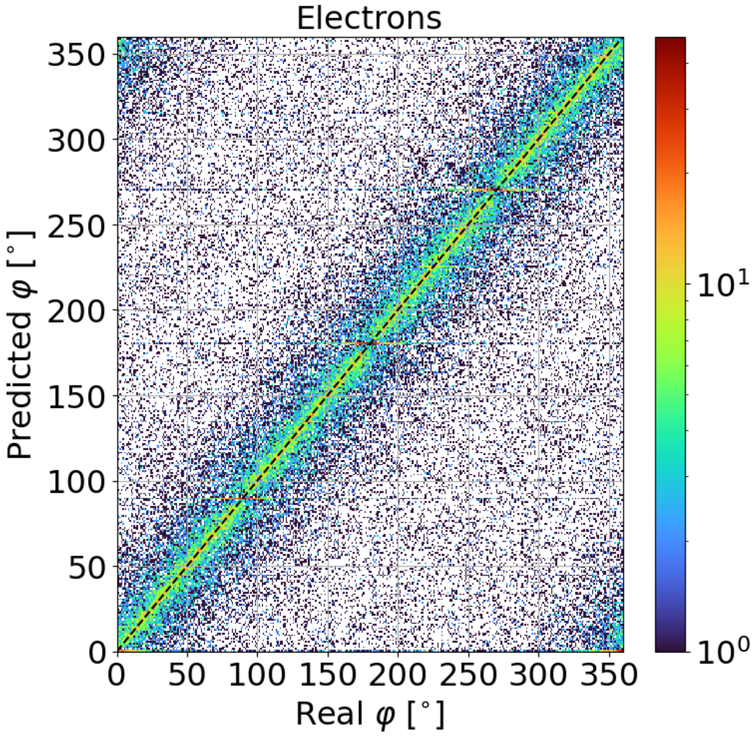

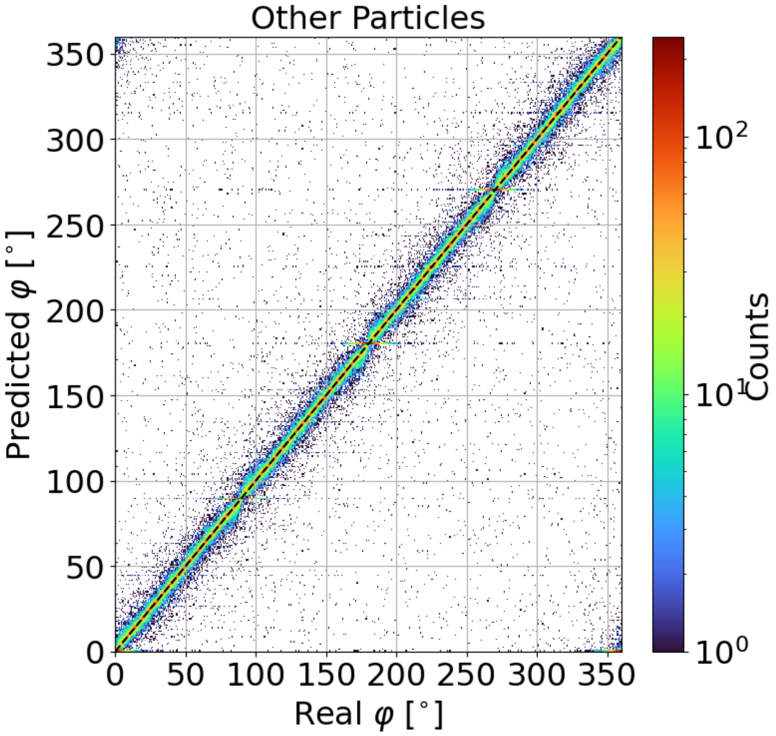

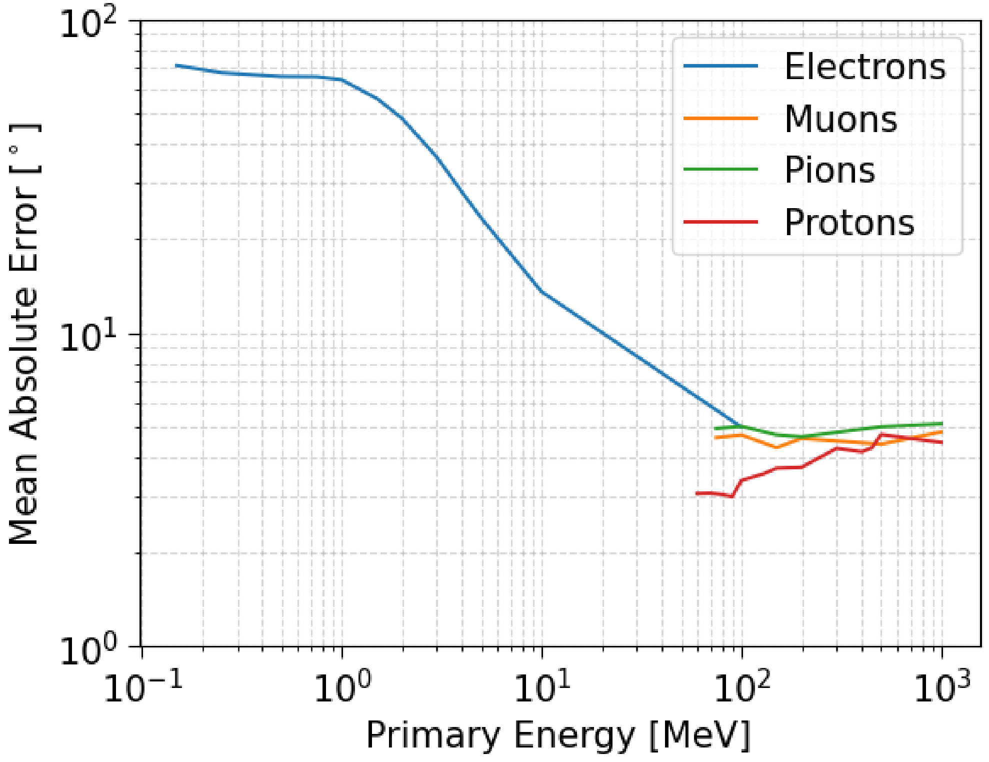

Rudimentary Classification

Particle tracks can be divided into two groups, with variable linearity and scattering:

1. **Lowly Ionising Particles (LIPs):**
   - ➪Electrons
   - ➪Photons
   - ➪Relativistic singly charged particles
2. **Medium Ionising Particles (MeIPs):**
   - ➪Protons <500 MeV
   - ➪Pions <200 MeV
   - ➪Muons <300 MeV
   - ➪Z>1 particles

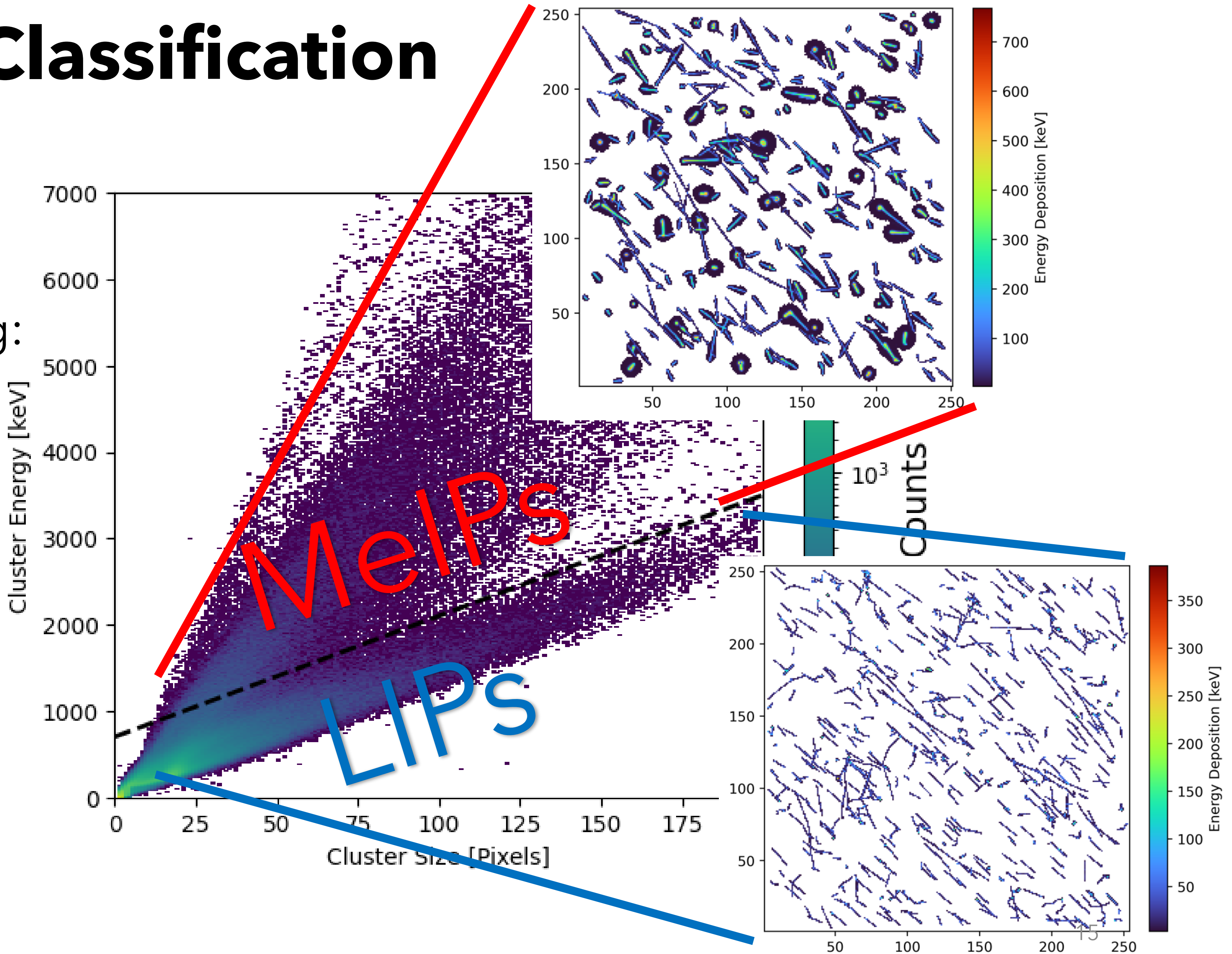

Field Directionality During Proton-Proton Collisions

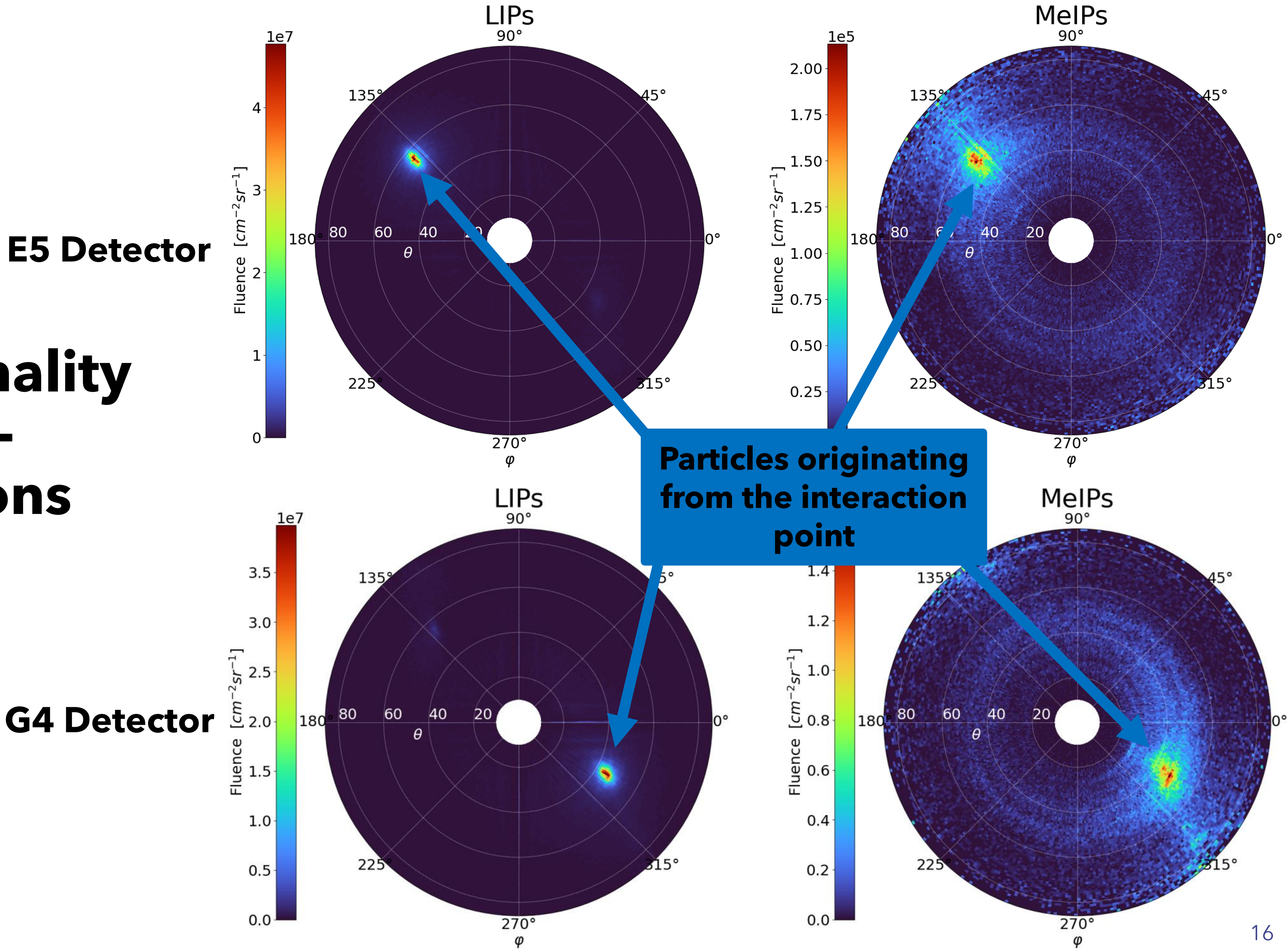

Field Directionality During Pb-Pb Collisions

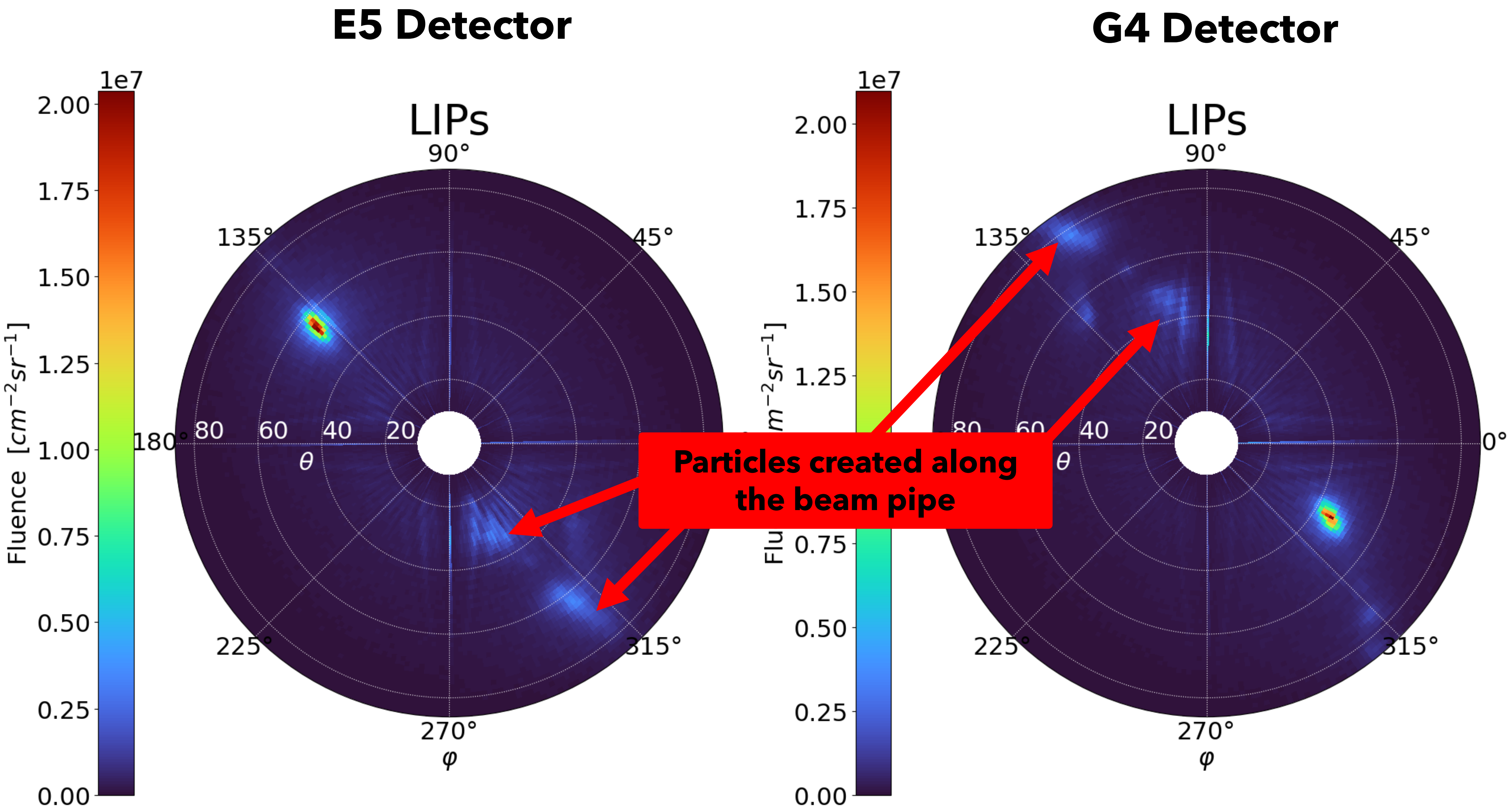

Time-Resolved Measurement of the Directionality Map Pb-Pb Collision Period

For increased accuracy only 5 minutes of data acquisition is need to produce reasonable statistics

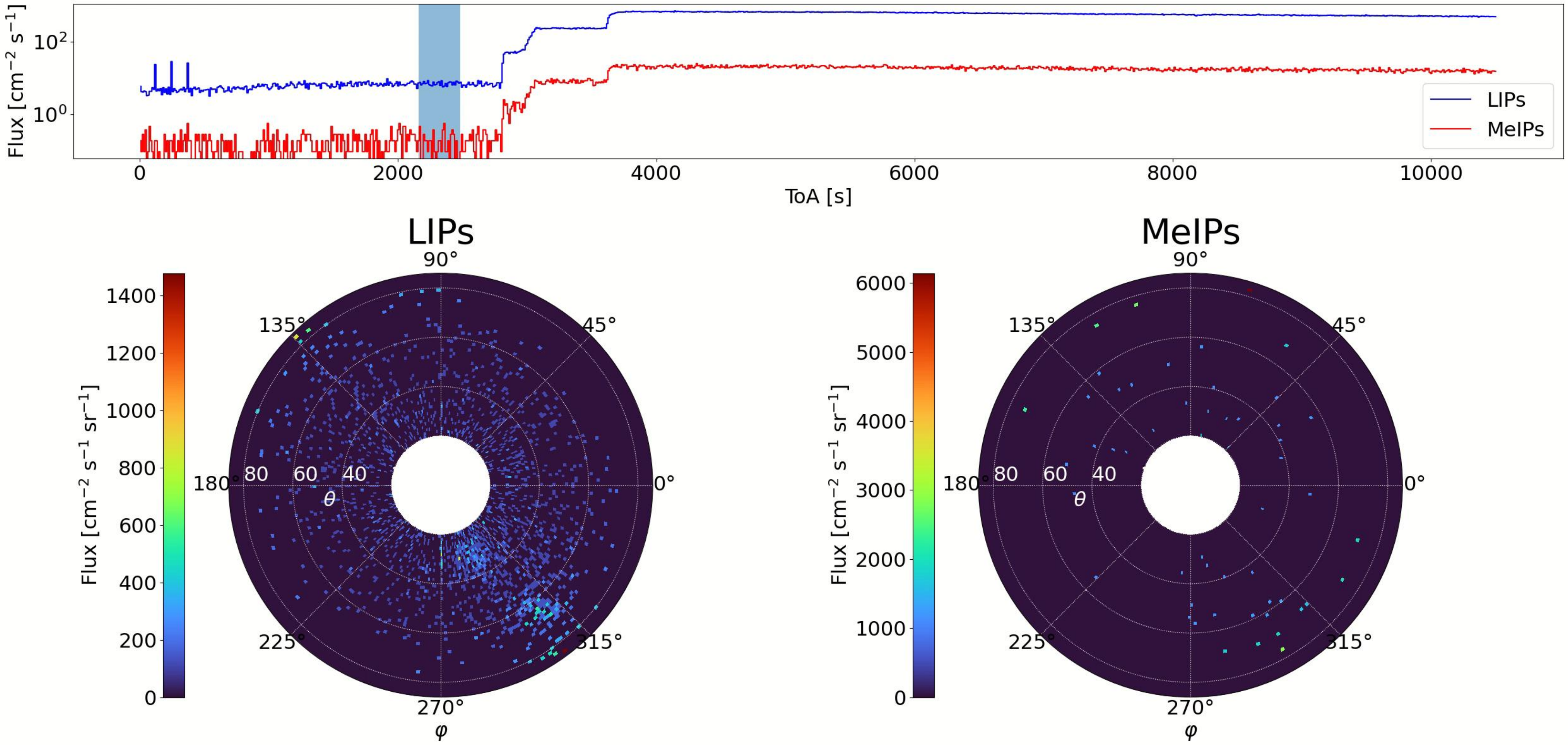

Radiation Field Decomposition According to Stopping Power

SATRAM And MOEDAL

A Brief Excursion:
Radiation Field Decomposition in Space

- Why the detour?
  - The mixed radiation field present in space has much lower complexity allowing us to more effectively develop and test algorithms for classification
- The data that will be used will come from the **S**pace **A**pplication **T**imepix **Ra**diation **M**onitor (**SATRAM**)
- The acquired knowledge can then be applied to the MoEDAL experiment

Space Application of Timepix Radiation Monitor (SATRAM)

- First Timepix in open space
- Power consumption of **2.5 W**
- Total mass **380 g** (107 x 70 x 55 mm)

Proba-V

- Minisatellite (158 kg)
- Altitude ~820 km (LEO)
- 101.21 minutes orbit duration
- Inclination 98.6°
- Sun-synchronous
- Launched 7th March 2013

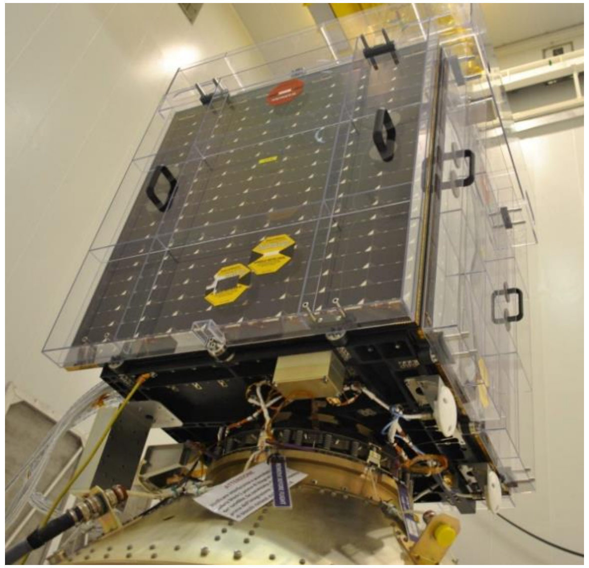

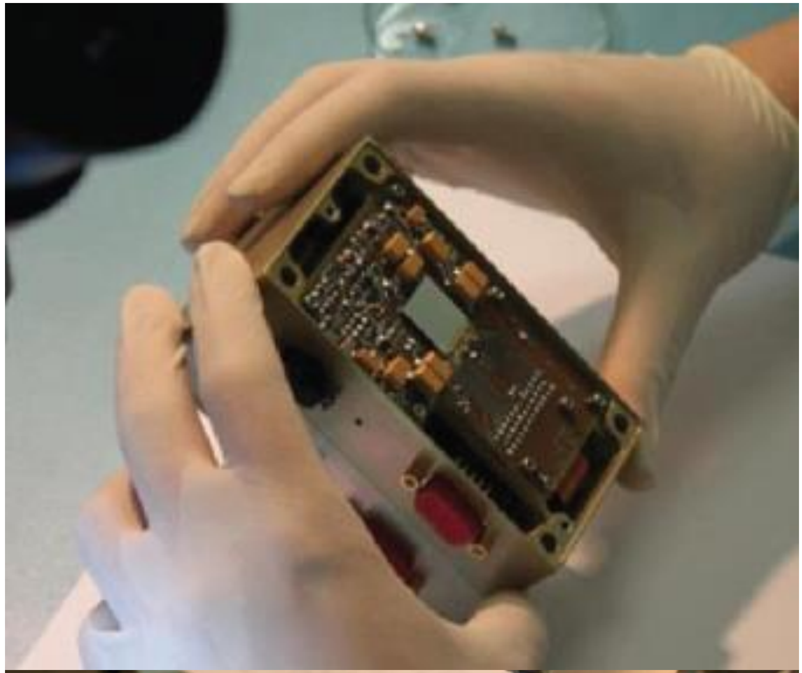

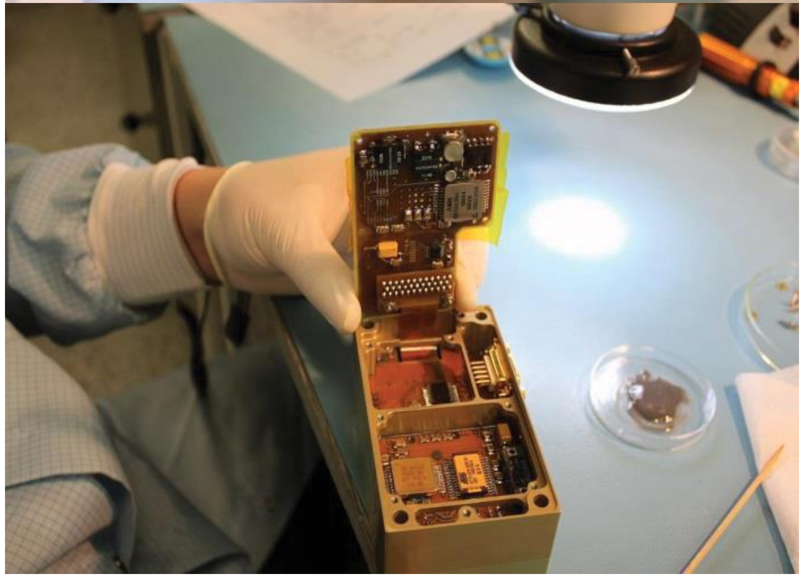

The Radiation Environment

Particle Spectrum:
E_p <400 MeV
E_e <7 MeV

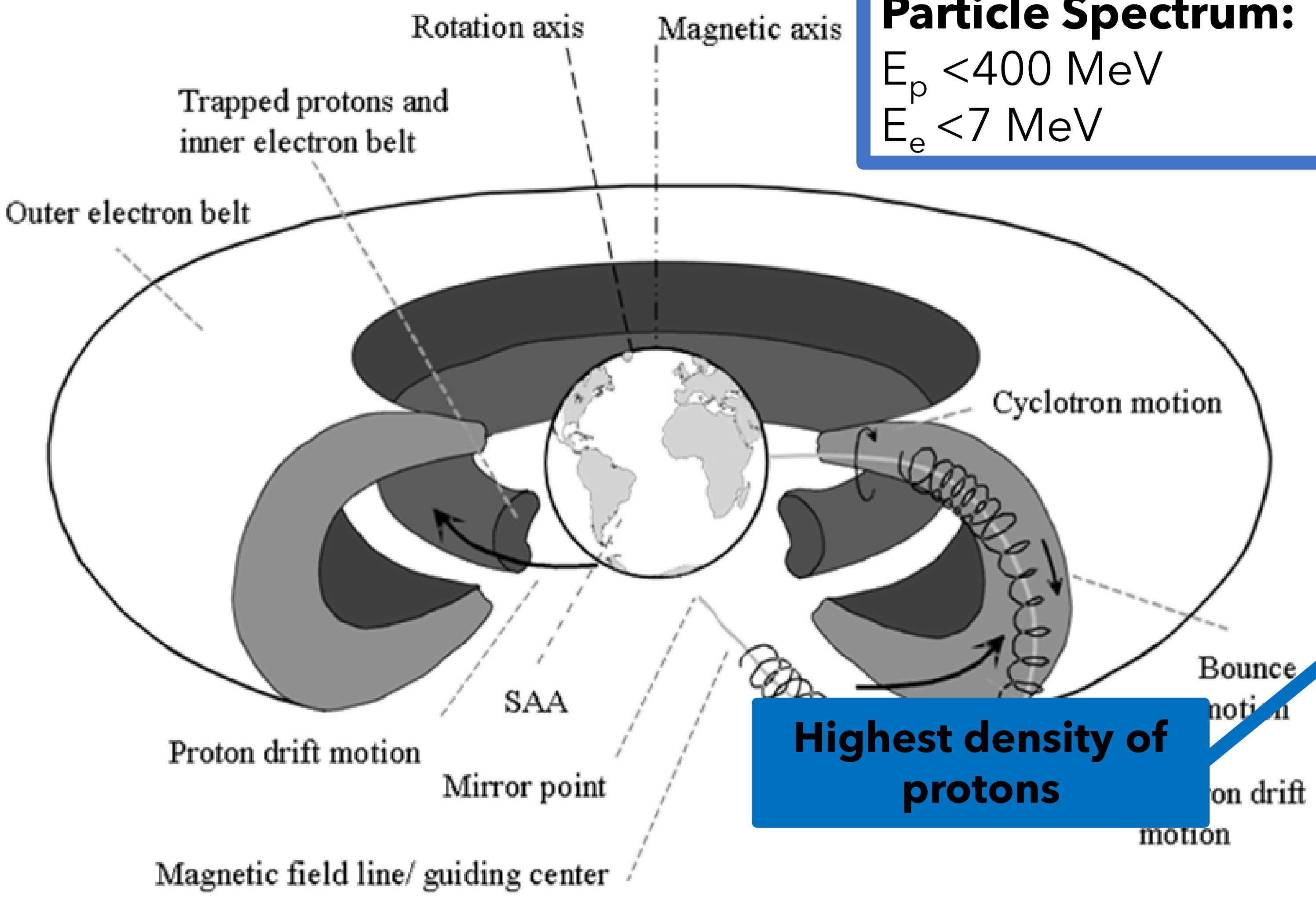

Highest density of protons

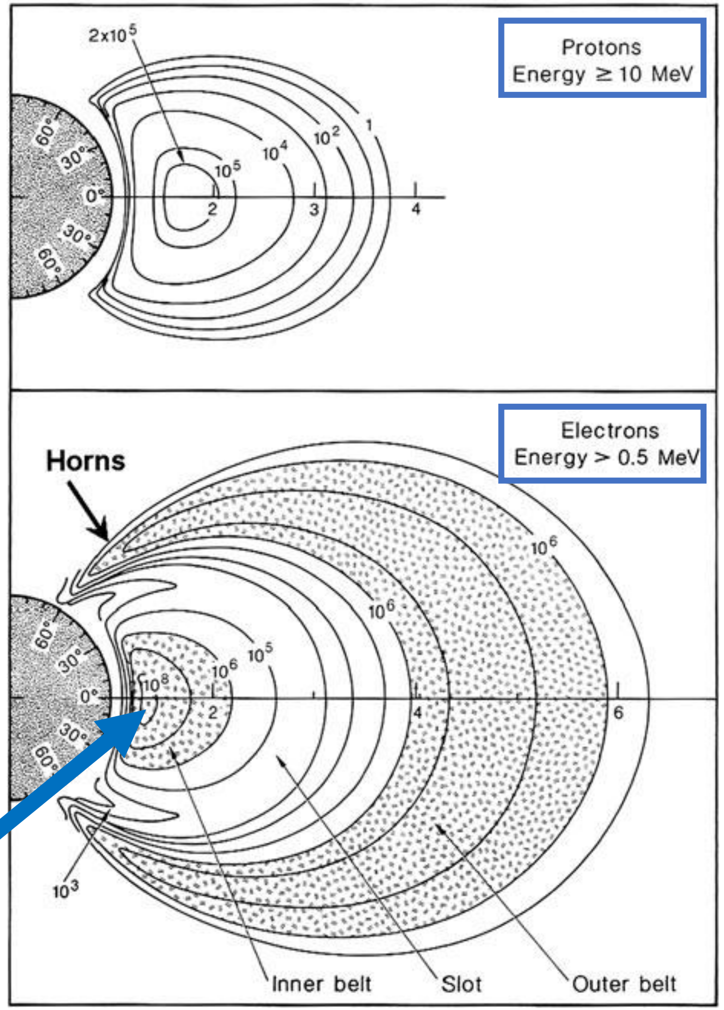

Mauk, B.H., Fox, N.J., Kanekal, S.G. et al. Space Sci Rev (2013) 179: 3.

https://satram.utef.cvut.cz/

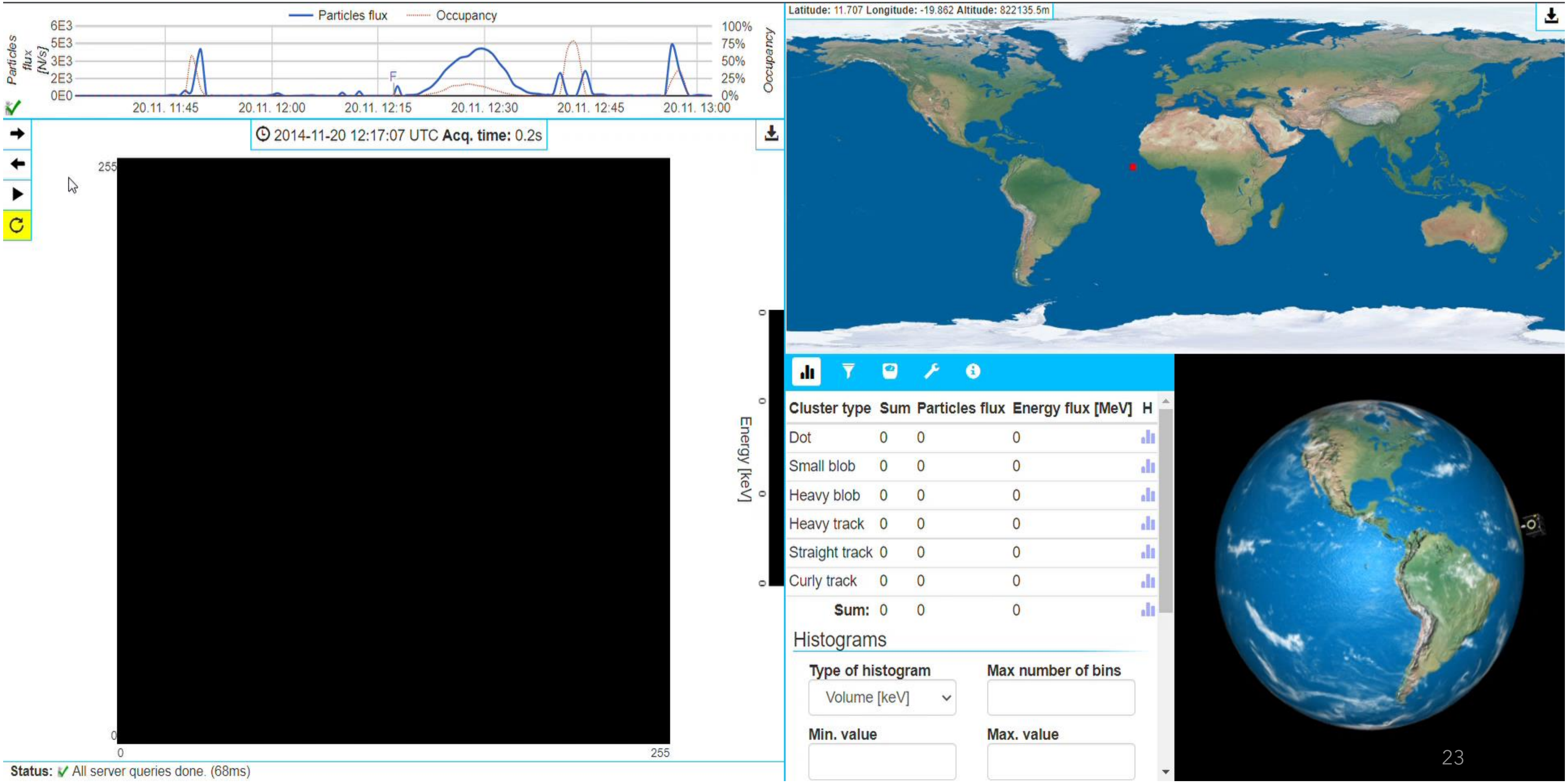

Particle Classification – Bayesian Deconvolution

This method works by decomposing the stopping power "signal" of the field into its contributing particle signals, from which the particle's distributions can be inferred

Response Matrix

$$n(E) = R\,\phi(C)$$

Measured dE/dx Spectrum

Particle Spectrum

$$R^T =$$

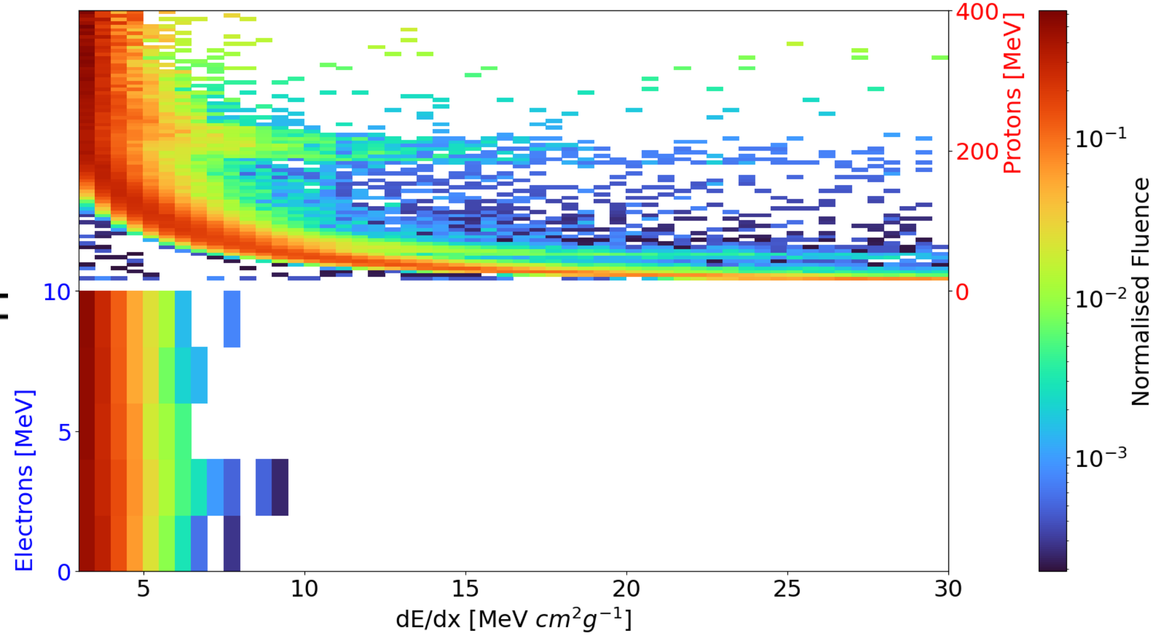

G. D'Agostini. Improved iterative Bayesian unfolding. 2010. https://doi.org/10.48550/arXiv.1010.0632

dE/dX and Particle Classification

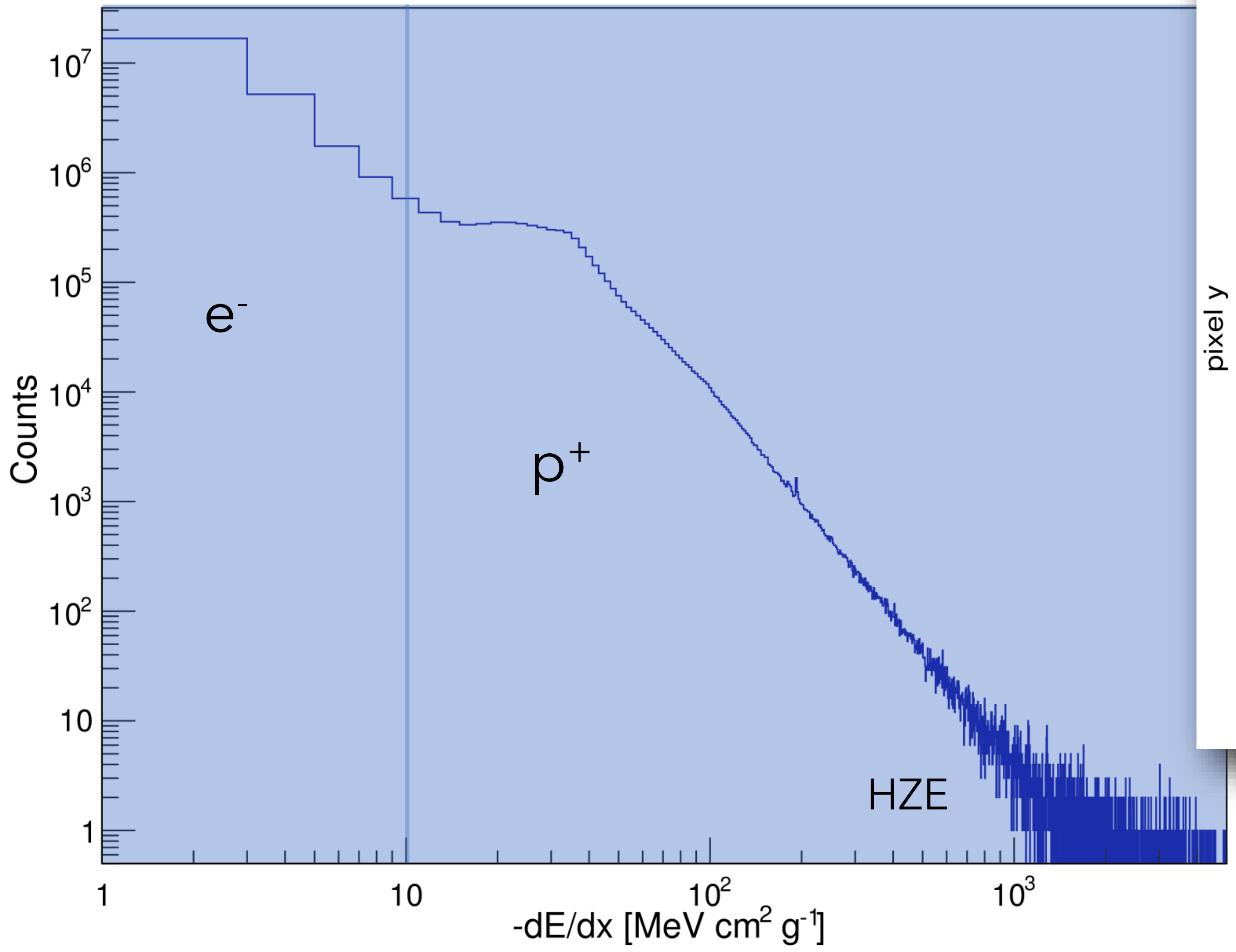

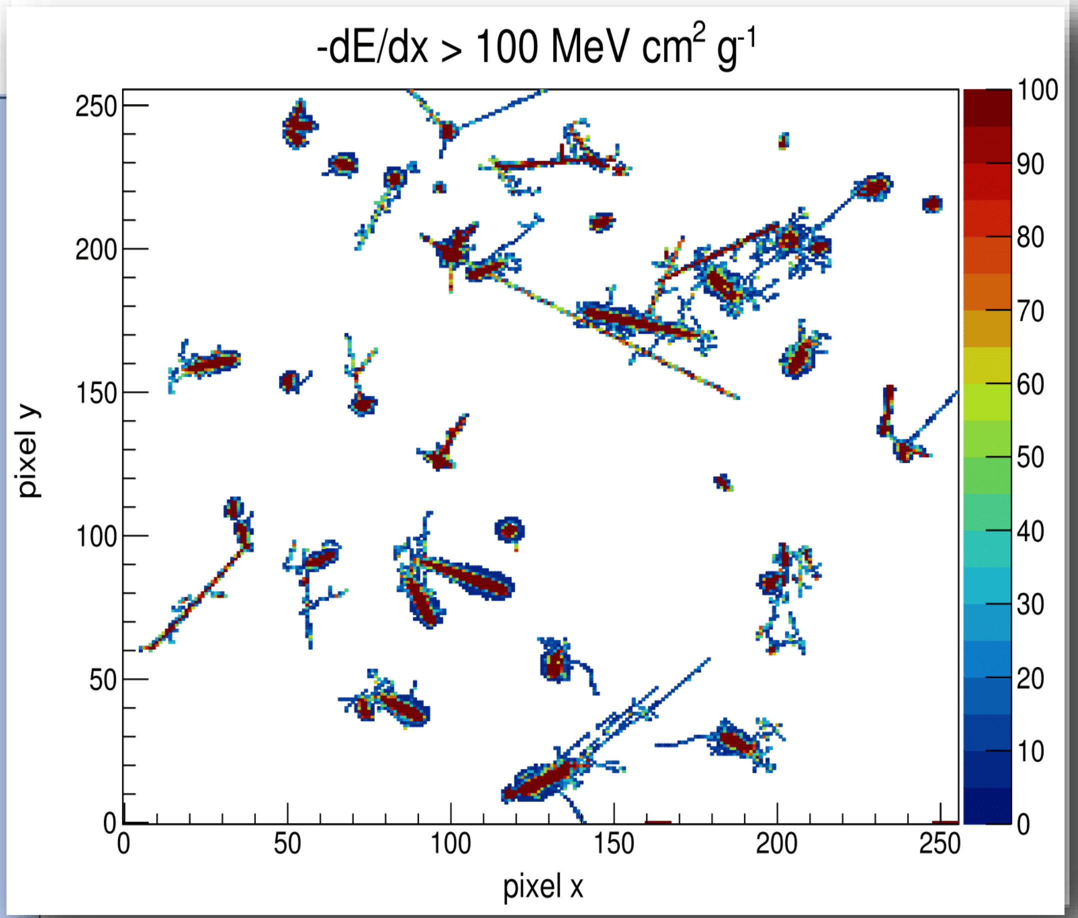

St. Gohl et al., "Study of the radiation fields in LEO with the Space Application of Timepix Radiation Monitor (SATRAM)", Advances in Space Research ***63****, Issue 5, pp. 1646-1660, (2019).*

Electron and Proton Flux Maps

e^- fluxes 3 orders of magnitude larger than p^+ fluxes

➡ Even small e^- misclassification distorts p^+ flux measurement

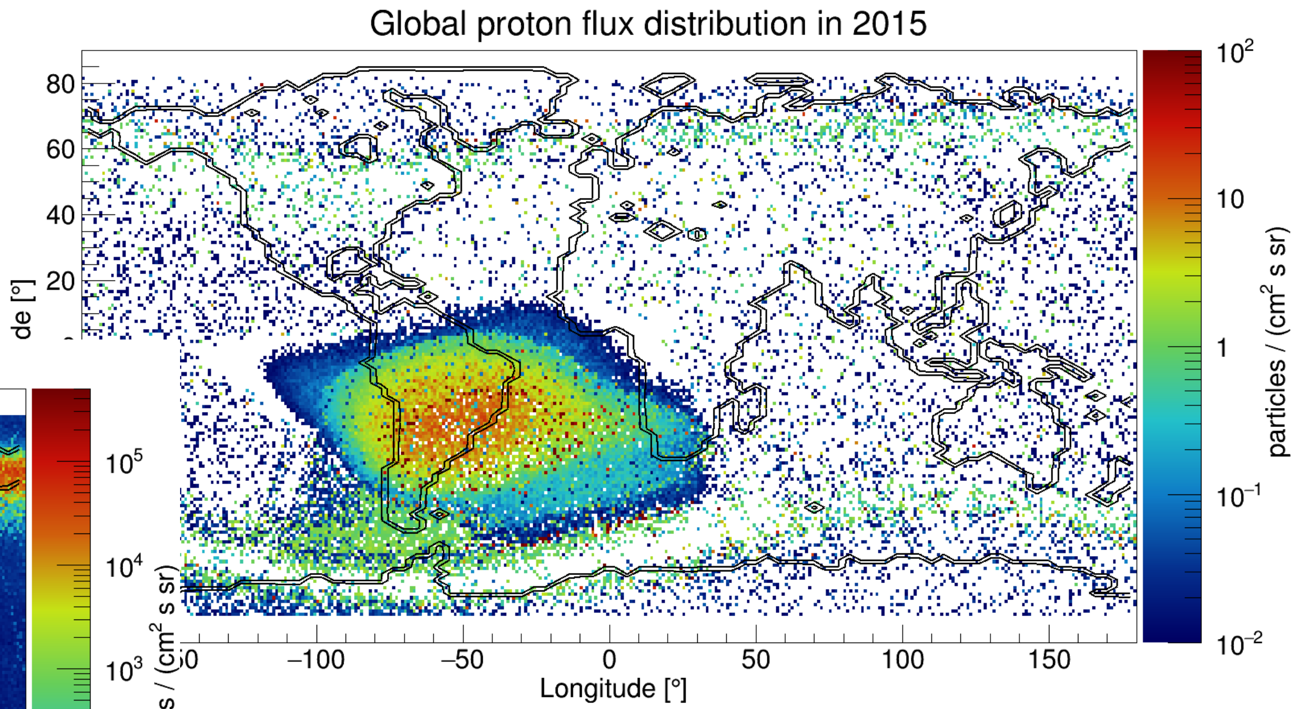

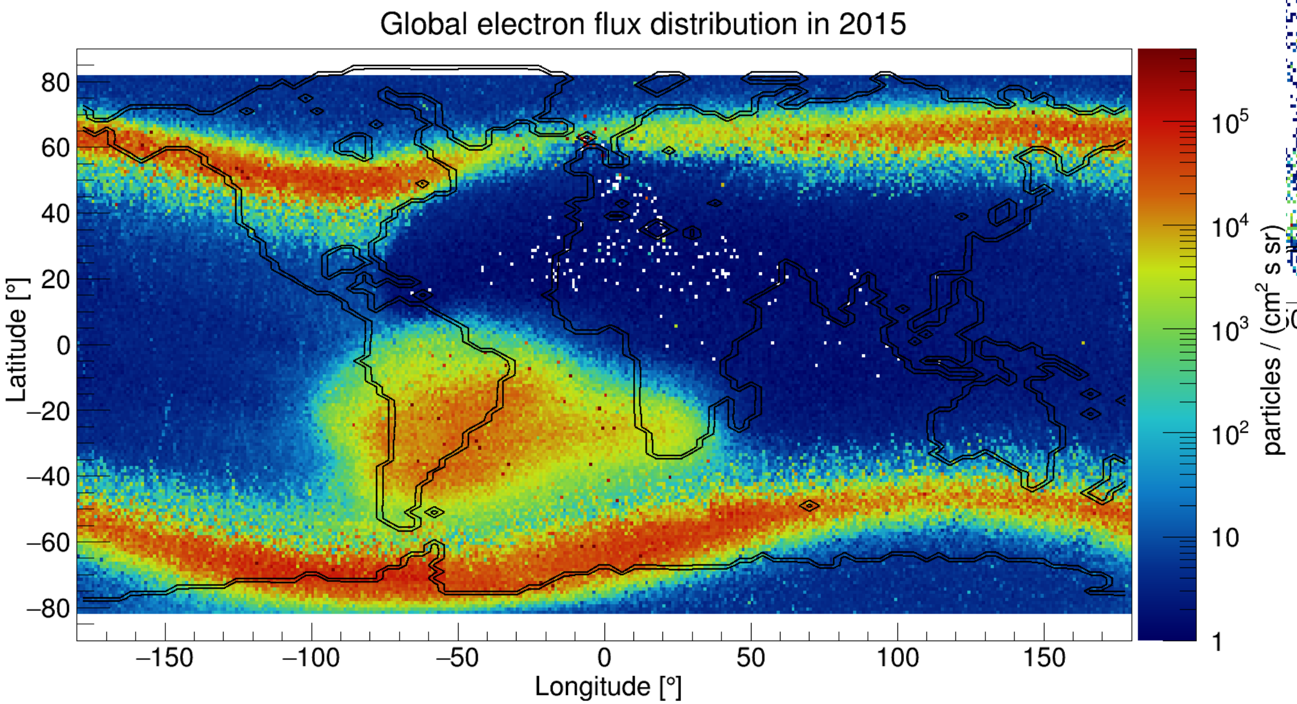

*St. Gohl et al., "Study of the radiation fields in LEO with the Space Application of Timepix Radiation Monitor (SATRAM)", Advances in Space Research **63**, Issue 5, pp. 1646-1660 (2019).*

First Measurement of the Trapped Proton Energy Spectrum with a Single-Layer Detector

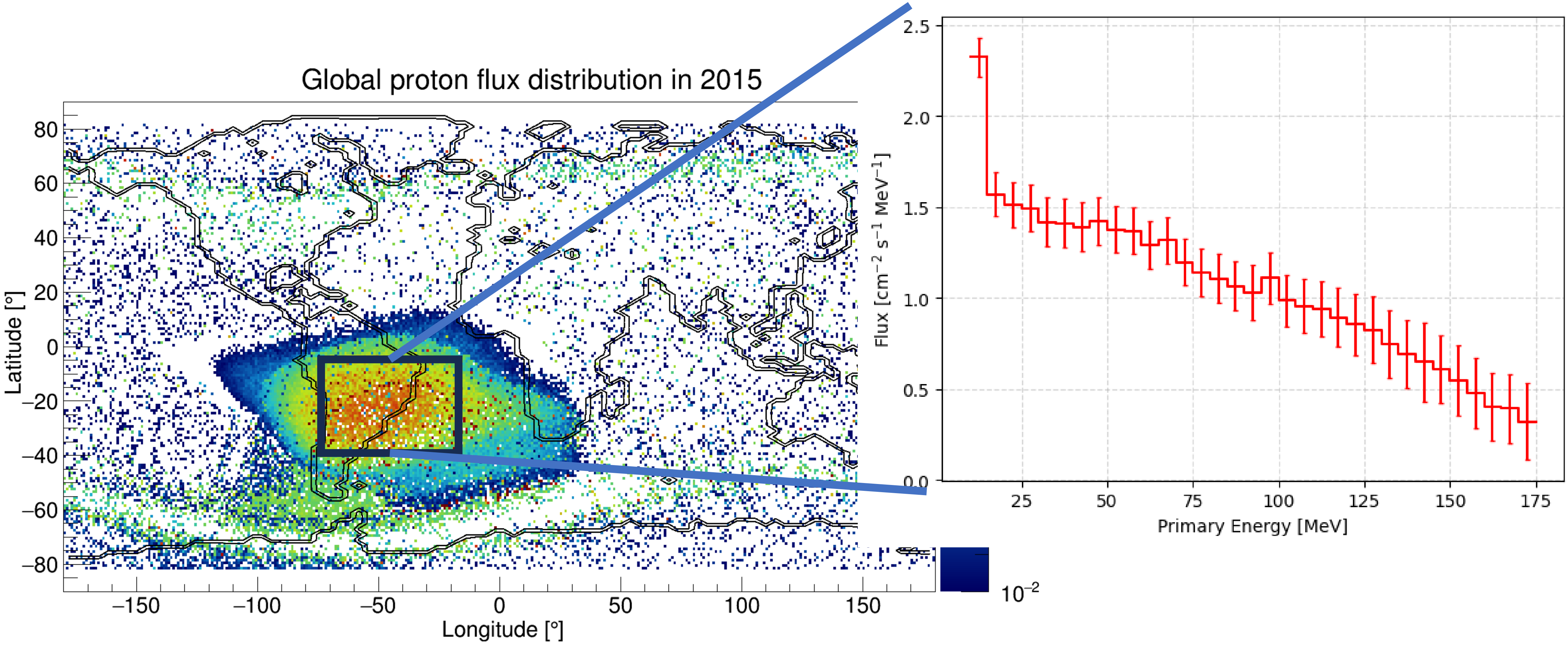

Stopping Power Classification at MoEDAL

A Closer look at Stopping Power

Region 1:
- ➩Electrons
- ➩Gammas
- ➩Singly charged relativistic particles

Region 2:
- ➩Protons <250 MeV
- ➩Pions <15 MeV
- ➩Muons <10 MeV

Regions 3:
- ➩Fragmentations
- ➩ Z>1 particles

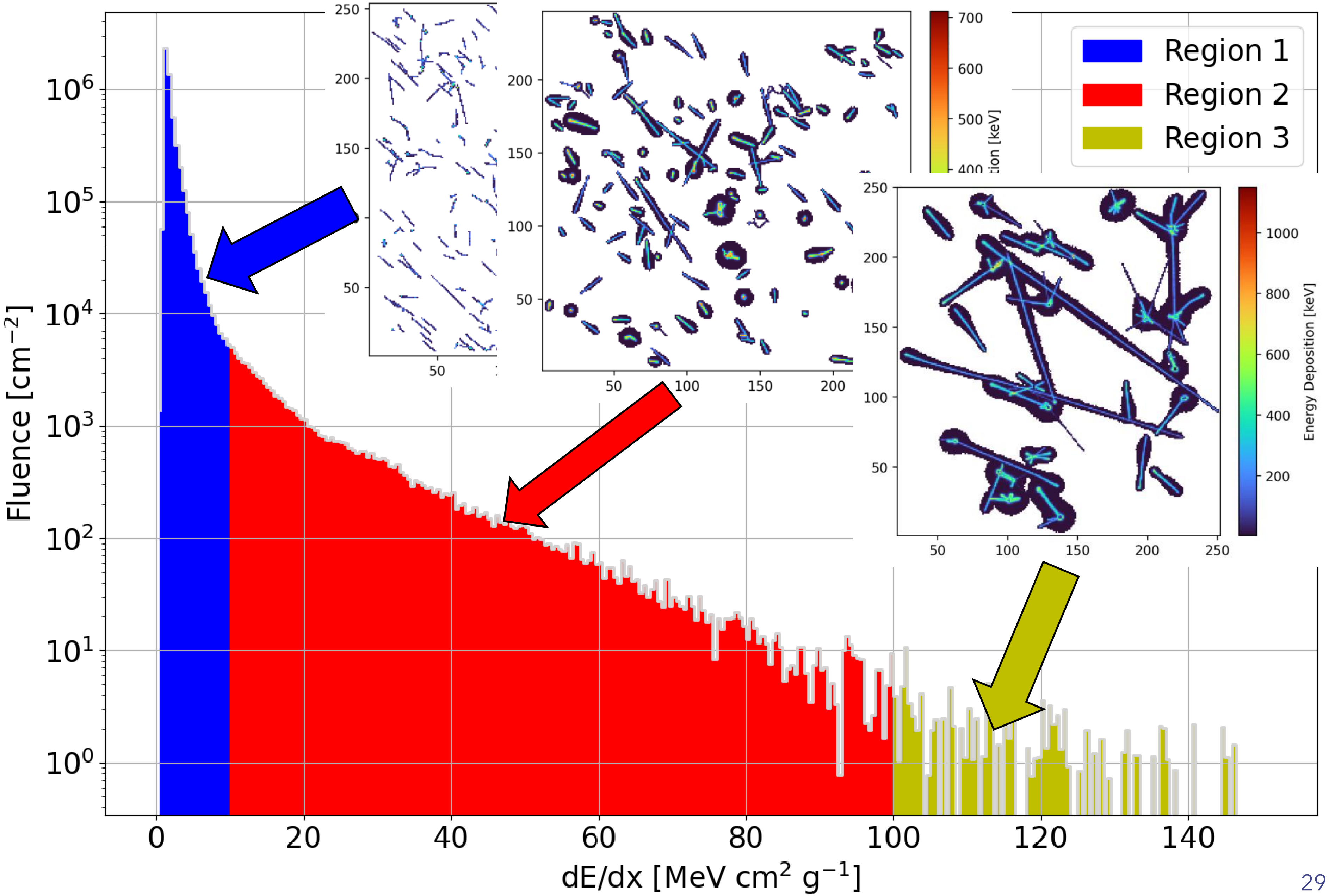

Conclusions

- 3D tracking
  - ➡ The capabilities of reconstructing particle trajectories from IP8 in real time and with single layer Timepix3 detectors have been demonstrated
- Stopping power and radiation field decomposition
  - ➡ The current are state-of-the-art algorithms in particle classification were shown and validated in the environment found in low earth orbit
  - ➡ Future work will be to improve particle classification by using advanced machine learning algorithms

Can we use Timepix3 in Search for the Avatars of New Physics?

$$\left\langle -\frac{dE}{dx} \right\rangle = Kz^2 \frac{Z}{A} \frac{1}{\beta^2} \left[\frac{1}{2} \ln \frac{2m_e c^2 \beta^2 \gamma^2 W_{\max}}{I^2} - \beta^2 - \frac{\delta(\beta\gamma)}{2} \right]$$

Highly charged energetic particles are known to produce distinct cluster pattern within Timepix3

Associated with:

- ⇨ High Stopping Power
- ⇨ Large number of delta rays

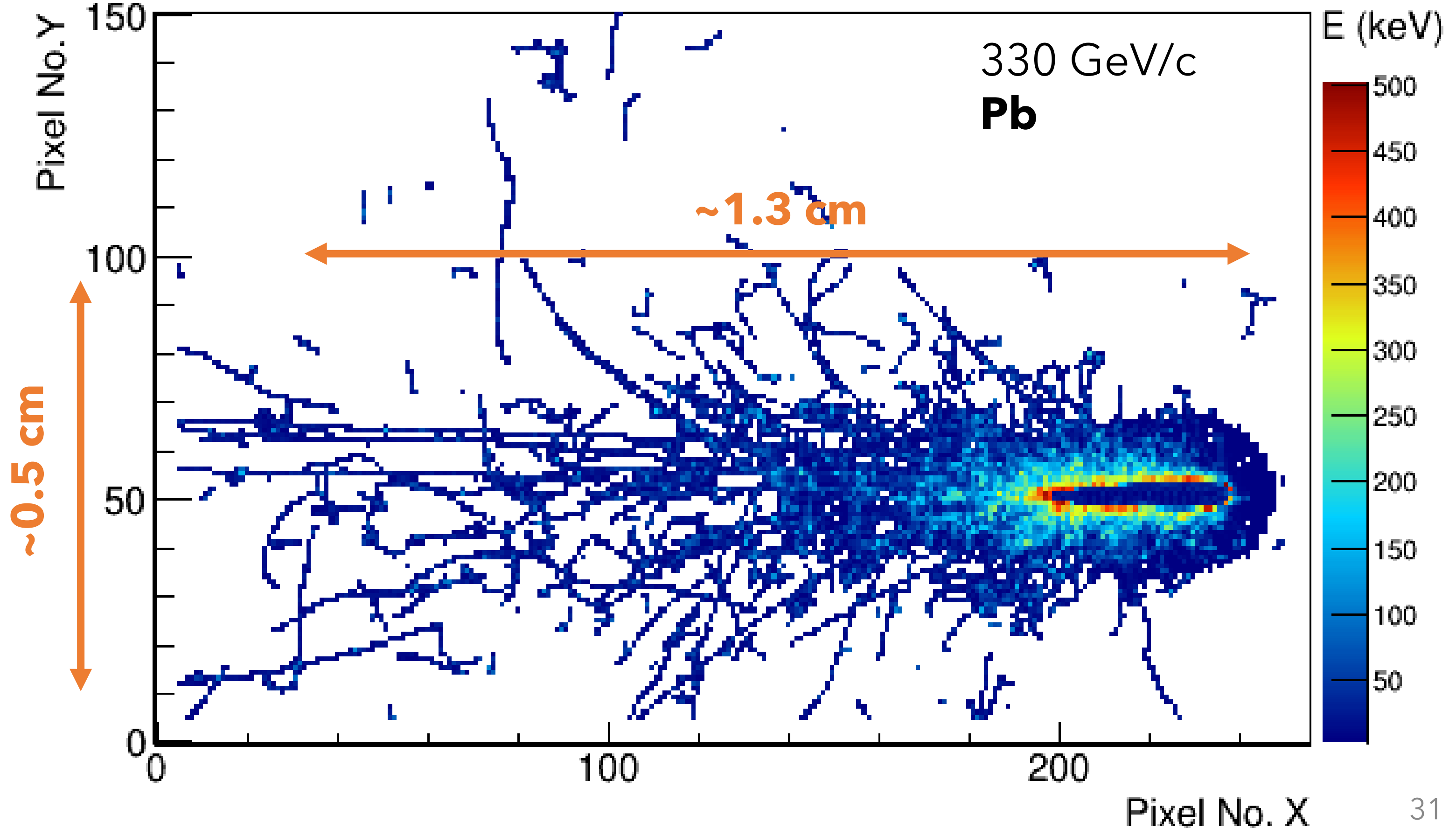

Thank you for your attention

This research was funded by the Czech Science Foundation grant number GM23-04869M.

Instruments for measurements in LEO

Next Generation Radiation Monitor (NGRM)

- Mass ~ 1 kg
- Consumption ~1-2 W

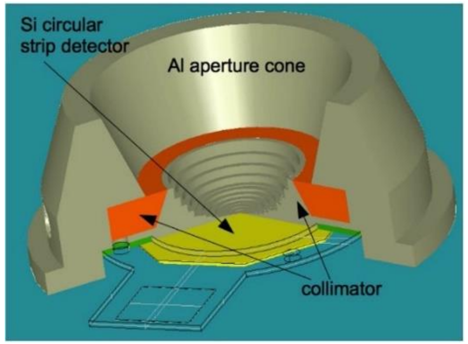

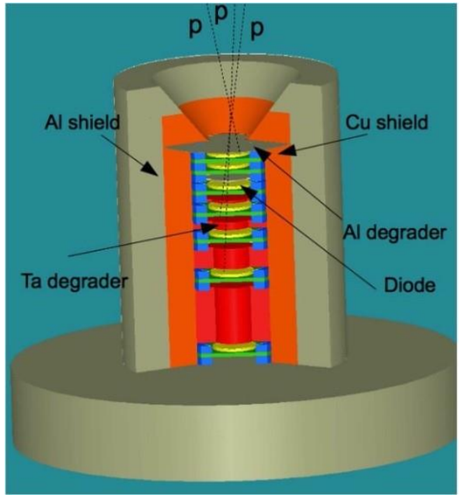

EPT (Energetic Particle Telescope)

- Mass: **4.6 kg**
- Consumption: 5.6 W

ICARE-NG:

- Mass: **2.4 kg**
- Consumption: 3 W

Particle Fluence

The formula was derived analytically to account for the removal of edge clusters

$$F = \sum_{i \in \{particles\}} \frac{d/cos(\theta_i)}{l \cdot d \cdot (l - d \cdot tan(\theta_i))}$$

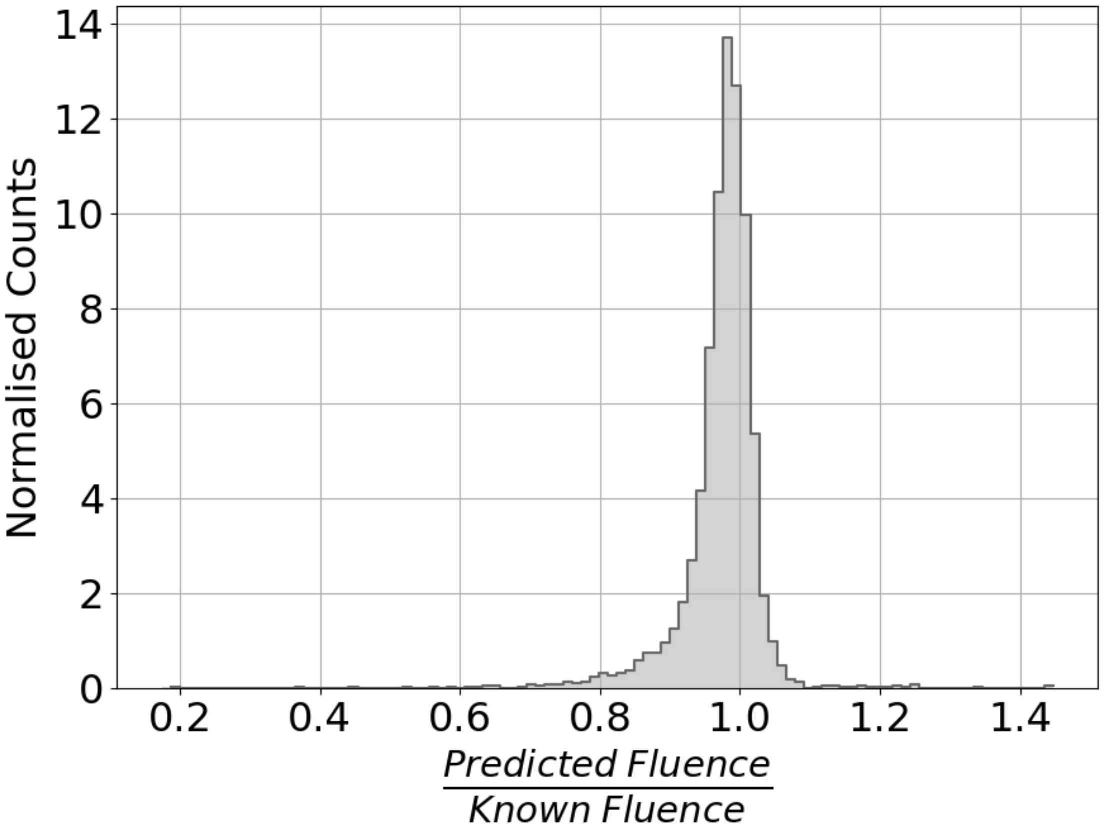

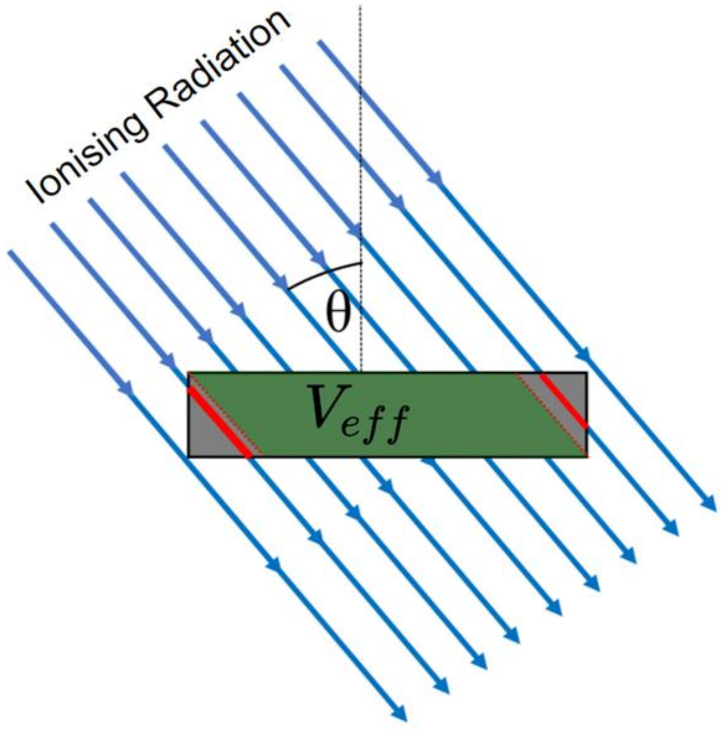

The new algorithm was tested in a Geant4 omnidirectional field simulation.

Testing Accuracy: 97%

Second Peak Localisation

- Follow correct alignment of the interaction of point
- It becomes possible to project the second peak in 3D space to determine its origin
- Projection shows the origin along the beam line further the theory of scattering beam due to wider beam

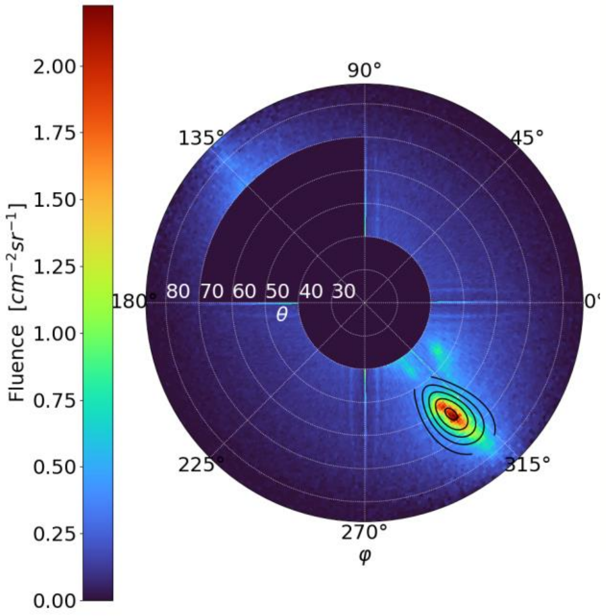

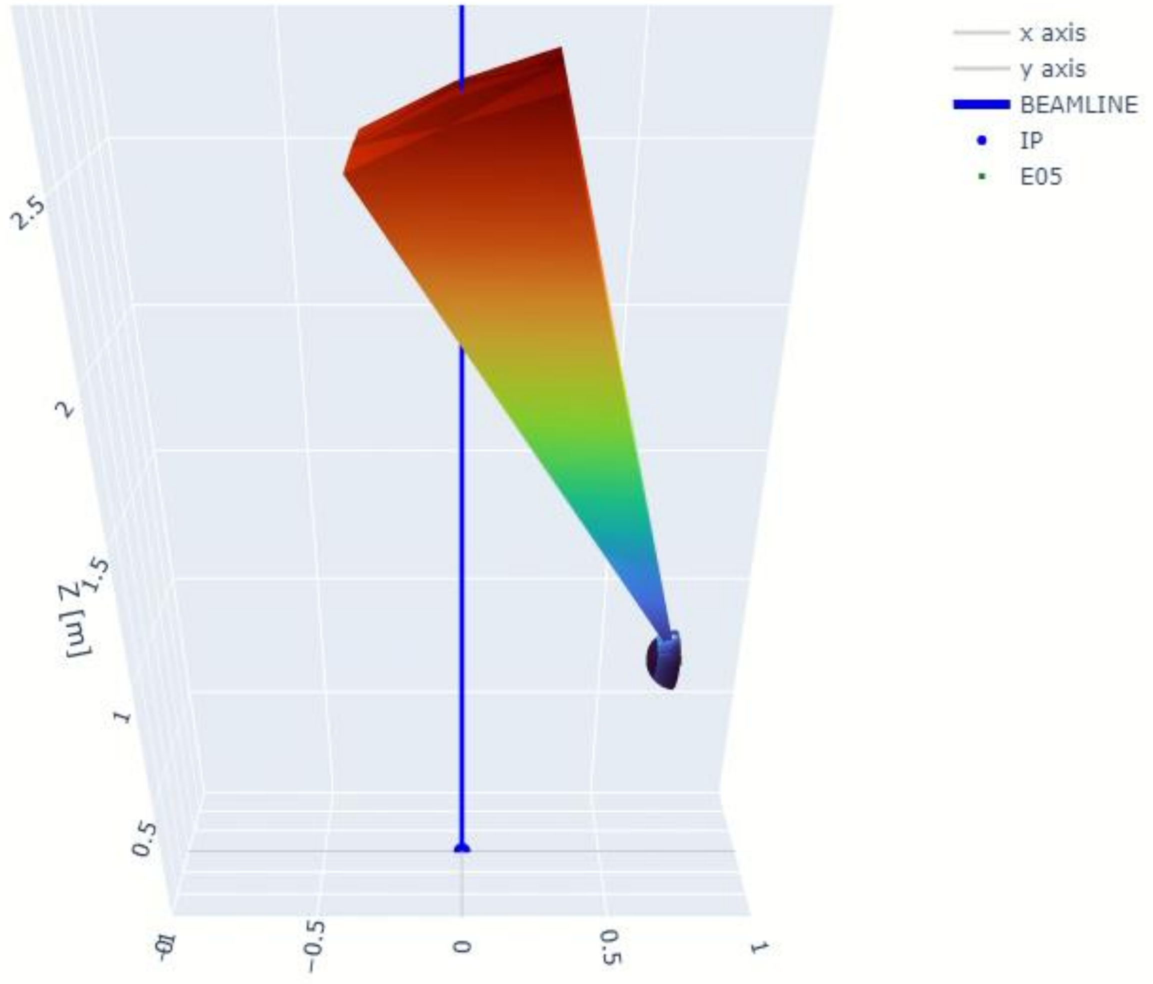

Bayesian Deconvolution Mathematical Background

Response Matrix

$$n(E) = R\,\phi(C)$$

Particle Spectrum

Measured dE/dx Spectrum

$$M \approx R^{-1} \Rightarrow \phi(C) = M\,n(E)$$

Bayesian Formula $\Rightarrow$ $$P(C_\mu|E_j) = \frac{P(E_j|C_\mu)\,P(C_\mu)}{\sum_\nu^{n_C} P(E_j|C_\nu)\,P(C_\nu)}$$

Probability of a cause (particle class present) given an effect (measurement)

$$\Rightarrow \phi(C_\mu) = \sum_{i=1}^{n_E} P(C_\mu|E_i)n(E_i)$$